Location and Emergency Inventory Pre-Positioning for Disaster Response Operations: Min-Max Robust Model and a Case Study of Yushu Earthquake

Wenjun Ni * Jia Shu † and Miao Song ‡

March 26, 2021

Abstract

Pre-positioning emergency inventory in selected facilities is commonly adopted to prepare for potential disaster threat. In this paper, we simultaneously optimize the decisions of facility location, emergency inventory pre-positioning, and relief delivery operations within a single-commodity disaster relief network. A min-max robust model is proposed to capture the uncertainties in both the left- and right-hand-side parameters in the constraints. The former corresponds to the proportions of the pre-positioned inventories usable after a disaster attack, while the latter represents the demands of the inventories and the road capacities in the disaster-affected areas. We study how to solve the robust model efficiently and analyze a special case that minimizes the deprivation cost. The application of the model is illustrated by a case study of the 2010 earthquake attack at Yushu County in Qinghai Province of PR China. The advantage of the min-max robust model is demonstrated through comparison with the deterministic model and the two-stage stochastic model for the same problem. Experiment variants also show that the robust model outperforms the other two approaches for instances with significantly larger scales.

*Department of Management Science and Engineering, School of Economics and Management, Southeast University. Email: niwenjun@connect.hku.hk

†Department of Management Science and Engineering, School of Economics and Management, Southeast University. Email: jshu@seu.edu.cn

‡Department of Logistics and Maritime Studies, Faculty of Business, The Hong Kong Polytechnic University. Email: miao.song@polyu.edu.hk

Keywords: disaster relief; facility location; network flow; inventory pre-positioning; min-max robust optimization

1 Introduction

Disasters can hardly be precisely predicted and have severe effects on human beings. For example, the 2010 Yushu earthquake in China caused 2,698 people killed, 11,000 injured, and 270 missing. The direct economic losses of the earthquake reached 22.85 billion yuan.[1] The massive-scale social and economic damages caused by disasters have brought increasing attention to the need for effective disaster relief management.

According to Altay and Green (2006), disaster operations management consists of four phases, i.e., mitigation, preparedness, response, and recovery. Mitigation and preparedness belong to pre-disaster relief actions that typically include facility location and emergency inventory pre-positioning (see, e.g., Toregas et al., 1971, Jia et al., 2007, Balcik and Beamon, 2008, Lee et al., 2009, Qi et al., 2010, Shu, 2010, Shen et al., 2011, Yushimito et al., 2012, Aboolian et al., 2013, Altay, 2013). Response and recovery are post-disaster relief actions, an important component of which is to deliver the emergency supplies (see, e.g., Haghani and Oh, 1996, Barbarosoğlu and Arda, 2004, Özdamar et al., 2004, Sheu, 2007, Tzeng et al., 2007, Campbell et al., 2008, Sheu, 2010, Huang et al., 2013). As pointed out by Tufekci and Wallace (1998), treating these pre- and post-event responses separately may result in suboptimality. This observation motivated the consideration of integrated location, inventory pre-positioning, and delivery for disaster relief in the recent literature (see, e.g., Mete and Zabinsky, 2010, Rawls and Turnquist, 2010, Salmerón and Apte, 2010, Campbell and Jones, 2011, Rawls and Turnquist, 2011, Bozorgi-Amiri et al., 2013, Davis et al., 2013, Dalal and Üster, 2017). We refer readers to Altay and Green (2006), Simpson and Hancock (2009), Galindo and Batta (2013), Anaya-Arenas et al. (2014), and Gupta et al. (2016) for excellent reviews in this area.

Due to the difficulty of predicting the timing and magnitude of a disaster, it is almost impossible to estimate the resulting damage to human life and infrastructure (cf. Barbarosoğlu and Arda, 2004). The node-wise disruption affects not only the demands of disaster relief commodities at the affected areas but also the availability of emergency supplies that are pre-positioned in certain

[1] Source: http://www.csi.ac.cn/manage/eqDown/dzzh/2010DiZhenZaiHai.html

facilities. The link-wise disruption may lead to partially functioning or totally unoperational roads. These disruptions create uncertainties on supply, demand, and road link capacity in disaster relief operations. Because of this stochastic nature, most integrated disaster relief response problems are formulated as a standard risk-neutral two-stage stochastic program. The pre- and post-disaster relief operations correspond to the first and second stages, respectively. The objective is to minimize the deterministic first stage cost plus the expectation of the stochastic second stage cost. Furthermore, the uncertainties are modeled using a finite number of scenarios, each of which happens with a known probability. Consequently, these models are commonly referred to as the scenario-based stochastic models. The study in Bozorgi-Amiri et al. (2013) is among the very few integrated disaster relief models that do not take the risk-neutral stochastic programming approach. Instead, a risk-averse two-stage stochastic program is proposed to minimize a linear trade-off between the expected cost of the two stages and the variance of the second stage cost. Nevertheless, this model also falls into the category of the scenario-based stochastic models as both the expectation and the variance are calculated based on given scenarios and their probabilities of happening.

These scenario-based models, although applied in various disaster relief management problems, face a major challenge in practical implementation, i.e., how to select the scenarios and calculate the probabilities for each scenario. To the best of our knowledge, in the disaster relief management literature, the only models that circumvent this difficulty by adopting a min-max criterion are contributed by Ben-Tal et al. (2011) and Najafi et al. (2013). Both of them focus on post-disaster operations. Furthermore, only the right-hand-side uncertainties are considered. In other words, the constraints in these models can be written in the form of $\mathbf{Ax} \leq \tilde{\mathbf{b}}$, where $\mathbf{x}$ represents the decision variables, $\mathbf{A}$ is a deterministic matrix, and $\tilde{\mathbf{b}}$ is a vector independent of $\mathbf{x}$ and subject to uncertainty.

In this paper, we complement the existing literature of disaster relief management by proposing a min-max robust model that integrates, in a disaster relief network, the decisions of facility location, emergency commodity pre-positioning, and transportation of emergency commodities to disaster-affected areas. The model captures both the node- and link-wise uncertainties, which are associated with the demand in each affected area, the proportion of usable inventory in each facility, and the capacity of each road link in the disaster relief network. As in the literature, we adopt the two-stage framework because the decisions span the pre- and post-disaster actions. However, instead of

modeling the uncertainties based on scenarios, we simply choose an "uncertainty set" within which the uncertain parameters may take values. The objective is then to minimize the sum of the first stage cost and the worst-case second stage cost among all possible realizations of the uncertain parameters falling into the uncertainty set. This approach is "robust" as it applies the min-max criterion to protect against all realizations in the uncertainty set. We note that this notion of robustness is different from the classical definition in, e.g., Soyster (1973) and Bertsimas and Sim (2004), where a solution is robust if it is feasible for any realization chosen from the uncertainty set. Unfortunately, as discussed in the second paragraph of Section 2.3, the classical definition of robustness cannot be applied to the disaster relief problem because a solution complying with this definition does not exist.

The main contributions of this paper can be summarized as follows:

- To the best of our knowledge, the proposed model is the first min-max robust model that considers both pre- and post-disaster operations in disaster relief management. Unlike the stochastic models, it does not require the joint distribution of the uncertain parameters. Instead, only the most likely values together with the upper and lower bounds of these random inputs are required. In addition, the level of conservatism of the robust model can be controlled through a parameter named the "uncertainty budget" to fit the attitude of the decision maker towards the worst-case outcome.

- Computationally tractable approaches are proposed to solve the robust model. This is non-trivial mainly because our model considers both left- and right-hand-side uncertainties. More specifically, the second stage problem of the proposed model contains equality constraints of the form $\tilde{\mathbf{A}}\mathbf{x}_1 + \mathbf{B}\mathbf{x}_2 = \tilde{\mathbf{b}}$, where $\mathbf{x}_1$ and $\mathbf{x}_2$ are the vectors for the first and second stage decision variables, $\mathbf{B}$ is a deterministic matrix, and both the matrix $\tilde{\mathbf{A}}$ and the vector $\tilde{\mathbf{b}}$ are subject to uncertainty. Also note that the literature, e.g., Ben-Tal et al. (2011) and Najafi et al. (2013), mainly focuses on the right-hand-side uncertainty, i.e., the randomness in $\tilde{\mathbf{b}}$.

- We study a special case of the proposed model that only considers the deprivation cost, which, as introduced by Holguín-Veras et al. (2013), represents the economic valuation of the human suffering incurred by the shortage of the emergency commodity in the post-disaster relief operations. For this simplified model, a closed-form optimal solution can be derived

under certain conditions. We obtain important insights on how to determine the uncertainty budget of the robust model through analyzing the closed-form solution.

- The min-max robust model is applied to a real-world earthquake relief case and its variants. Extensive numerical results reveal that the min-max robust model outperforms both the deterministic model and the two-stage stochastic model, demonstrating that the min-max robust model provides a practical decision-making tool for disaster relief operations.

The remainder of this paper is organized as follows. In Section 2, we present a min-max robust model for the integrated location and emergency inventory pre-positioning problem that captures uncertainties in demands, proportions of usable inventories, and road link capacities. Section 3 is devoted to discuss how to solve the robust model efficiently and analyze the special case that minimizes the deprivation cost. We use a case study in Section 4 and its variants in Section 5 to illustrate the application of the model and demonstrate the advantage of the min-max robust model. Finally, the paper is concluded in Section 6.

2 Model Formulation

We consider a single-commodity network for the distribution of emergency supplies, e.g., humanitarian relief commodity packages that may contain water, food, medical kits, tents, clothes, etc., in case of a disaster event. A total amount of these emergency supplies, denoted by R, is given by the pre-disaster recovery plan. The corresponding distribution network is characterized by an undirected graph $\mathcal{G}(N, A)$, where $N = \{1, 2, \ldots, n\}$ and $A = \{(i, j) : i, j \in N\}$ denote the set of the nodes and the set of the links of $\mathcal{G}(N, A)$, respectively. Each node in N corresponds to a potential demand area for disaster relief. It also represents a potential facility site to store the pre-positioned emergency supplies, which has a given capacity M_i for any $i \in N$. After the occurrence of a disaster, the pre-positioned supplies are sent from the open facilities to the demand areas via the links in A.

In the pre-disaster operations, we need to decide where to set up the facilities for pre-positioning emergency supplies and how much inventory to be pre-positioned in each open facility. Following the nomenclature in the two-stage stochastic program, these pre-disaster decisions are referred to as the first stage decisions and represented by the decision variables in Table 1. To simplify the

notation, we denote them by the vectors $\mathbf{y}$ and $\mathbf{r}$, respectively. Obviously, the first stage decisions are feasible as long as

$$\sum_{i \in N} r_i = R, \tag{1}$$

$$0 \leq r_i \leq M_i y_i, \qquad \forall i \in N, \tag{2}$$

$$y_i \in \{0, 1\}, \qquad \forall i \in N. \tag{3}$$

Constraint (1) specifies that the total amount of the emergency supplies is R, while the second inequality in constraint (2) ensures that inventories can only be stored in the open facilities and are subject to the capacity constraints. These first stage decisions are associated with fixed facility costs and variable commodity handling costs, which are also shown in Table 1. As a result, the first stage cost, i.e., the pre-disaster cost, is $\sum_{i \in N} F_i y_i + \sum_{i \in N} h_i r_i$.

Table 1: First stage decision variables and cost parameters

First stage decision variables	
y_i	binary variable that equals 1 if facility i opens and 0 otherwise, for each $i \in N$
r_i	amount of the emergency inventory pre-positioned at node i, for each $i \in N$
First stage cost parameters	
F_i	fixed cost of locating and operating a facility at node i, for each $i \in N$
h_i	per unit commodity handling cost at node i, for each $i \in N$, which includes the cost to purchase, transport, and store one unit of the commodity in the pre-disaster actions

As mentioned in Section 1, due to the node- and link-wise disruptions caused by a disaster, the amount of the emergency commodities demanded by each node, the proportion of the pre-positioned inventory that remains usable at each open facility, and the link capacity available to ship the commodities are all subject to uncertainty. These parameters are listed in Table 2 and can only be realized after the occurrence of a disaster. For simplicity, the uncertain vectors $\tilde{\mathbf{d}}$, $\tilde{\boldsymbol{\rho}}$, and $\tilde{\mathbf{u}}$ are adopted to represent $\tilde{d}_i$, $\tilde{\rho}_i$, and $\tilde{u}_{ij}$ for any $i \in N$ and $(i, j) \in A$, respectively.

Based on the first stage decisions $(\mathbf{y}, \mathbf{r})$ and the realizations of the random parameters $(\tilde{\mathbf{d}}, \tilde{\boldsymbol{\rho}}, \tilde{\mathbf{u}})$, we can plan the post-disaster operations, which are referred to as the second stage decisions. The corresponding decision variables and the associated costs are shown in Table 3. Again, for brevity,

Table 2: Uncertain parameters realized after the occurrence of a disaster

$\tilde{d}_i$	random demand of the emergency commodities at node i after a disaster, $\forall i \in N$
$\tilde{\rho}_i$	random proportion of the commodities pre-positioned at node i that are usable in disaster relief, $\forall i \in N$
$\tilde{u}_{ij}$	random capacity on link (i,j) available for disaster relief, $\forall (i,j) \in A$

we use $\mathbf{x}$, $\mathbf{z}^+$, and $\mathbf{z}^-$ to represent the vectors of the decision variables x_{ij} for all $(i,j) \in A$, z_i^+ for all $i \in N$, and z_i^- for all $i \in N$, respectively. Using these notations, the optimized second stage cost, i.e., the post-disaster cost, can be obtained by

$$\begin{aligned} \mathcal{Q}(\mathbf{r}, \tilde{\mathbf{d}}, \tilde{\boldsymbol{\rho}}, \tilde{\mathbf{u}}) \quad = \quad & \min_{\mathbf{x},\mathbf{z}^+,\mathbf{z}^-} \quad \sum_{(i,j)\in A} c_{ij}x_{ij} + \sum_{i\in N}(q_i^+ z_i^+ + q_i^- z_i^-) \\ & \text{s.t.} \quad \tilde{\rho}_i r_i + \sum_{j:(j,i)\in A} x_{ji} - \sum_{j:(i,j)\in A} x_{ij} - z_i^+ + z_i^- = \tilde{d}_i, \quad \forall i \in N, \\ & \qquad 0 \le x_{ij} \le \tilde{u}_{ij}, \qquad \forall (i,j) \in A, \\ & \qquad z_i^+, z_i^- \ge 0, \qquad \forall i \in N, \end{aligned} \tag{4}$$

where the first constraint represents flow conservation.

Based on the above description, Sections 2.1, 2.2, and 2.3 formulate the deterministic, stochastic, and min-max robust models for location and inventory pre-positioning in disaster relief management, respectively.

2.1 Deterministic Model

The deterministic model assumes that there is no uncertainty associated with $(\tilde{\mathbf{d}}, \tilde{\boldsymbol{\rho}}, \tilde{\mathbf{u}})$. To distinguish from the uncertain parameters, we denote the deterministic counterpart by $(\mathbf{d}, \boldsymbol{\rho}, \mathbf{u})$. The deterministic model can then be formulated as

$$\begin{aligned} \min_{\mathbf{y},\mathbf{r}} \quad & \sum_{i\in N} F_i y_i + \sum_{i\in N} h_i r_i + \mathcal{Q}(\mathbf{r}, \mathbf{d}, \boldsymbol{\rho}, \mathbf{u}) \\ \text{s.t.} \quad & (1), (2), (3), \end{aligned} \tag{5}$$

where $\mathcal{Q}(\mathbf{r}, \mathbf{d}, \boldsymbol{\rho}, \mathbf{u})$ is defined in (4).

Table 3: Second stage decision variables and cost parameters

Second stage decision variables	
x_{ij}	flow quantity across link (i,j), for each $(i,j) \in A$
z_i^+	quantity of the unused inventory at node i, for each $i \in N$
z_i^-	quantity of the unsatisfied demand at node i, for each $i \in N$
Second stage cost parameters	
c_{ij}	per unit transportation cost across link (i,j), for each $(i,j) \in A$
q_i^+	penalty cost for each unit of unused commodity at node i, for each $i \in N$, which corresponds to the extra inventory holding or disposal cost
q_i^-	penalty cost for each unit of unsatisfied demand at node i, for each $i \in N$, which represents the deprivation cost, i.e., the economic measure of human suffering associated with shortage (cf. further discussions in Section 3.4), and/or the cost of getting additional supply from the unaffected areas

2.2 Two-Stage Stochastic Model

The two-stage stochastic model minimizes the first stage cost plus the expectation of the second stage cost. The joint distribution of $(\tilde{\mathbf{d}}, \tilde{\boldsymbol{\rho}}, \tilde{\mathbf{u}})$ are required to compute the expectation of the second stage cost. In most cases, a (finite) set of scenarios denoted by S is considered. Each of them happens with a probability p_s for any $s \in S$. Applying these notations, we obtain the following two-stage stochastic model:

$$\begin{aligned} \min_{\mathbf{y},\mathbf{r}} \quad & \sum_{i \in N} F_i y_i + \sum_{i \in N} h_i r_i + \sum_{s \in S} p_s \mathcal{Q}(\mathbf{r}, \mathbf{d}^s, \boldsymbol{\rho}^s, \mathbf{u}^s) \\ \text{s.t.} \quad & (1), (2), (3), \end{aligned} \tag{6}$$

where $\mathcal{Q}(\mathbf{r}, \mathbf{d}^s, \boldsymbol{\rho}^s, \mathbf{u}^s)$ for any $s \in S$ is defined in (4), i.e., the instance of the optimization problem $\mathcal{Q}(\mathbf{r}, \tilde{\mathbf{d}}, \tilde{\boldsymbol{\rho}}, \tilde{\mathbf{u}})$ in (4) for the given $\mathbf{y}$ and the possible outcome $(\mathbf{d}^s, \boldsymbol{\rho}^s, \mathbf{u}^s)$ of $(\tilde{\mathbf{d}}, \tilde{\boldsymbol{\rho}}, \tilde{\mathbf{u}})$. Although model (6) does not explicitly have the second stage decisions for each scenario $s \in S$, the instance of $\mathcal{Q}(\mathbf{r}, \mathbf{d}^s, \boldsymbol{\rho}^s, \mathbf{u}^s)$ yields an optimal second stage solution that exclusively corresponds to the second stage decisions for scenario s. In other words, model (6) allows different scenarios having different second stage decisions. We also note that model (6) can be viewed as a single-commodity version

of the model proposed in Rawls and Turnquist (2010).

2.3 Min-Max Robust Model

As mentioned before, it is very challenging to determine the scenarios as well as the corresponding probabilities in model (6). To address this issue, we propose the corresponding min-max robust model.

Suppose that the uncertain vectors $\tilde{\mathbf{d}}$, $\tilde{\boldsymbol{\rho}}$, and $\tilde{\mathbf{u}}$ in the second stage can take any values in the uncertainty sets D, P, and U, respectively. The classical robust optimization model, e.g., that in Soyster (1973) and Bertsimas and Sim (2004), makes all decisions at the same time epoch and so can be viewed as a single-stage problem. Given the uncertainty set for the uncertain parameters, a solution is robust if it is feasible for any realization of these uncertain parameters chosen from the uncertainty set. Casting our problem into this framework, we would like to get a solution $(\mathbf{y}, \mathbf{r}, \mathbf{x}, \mathbf{z}^+, \mathbf{z}^-) \in \mathbb{R}^{4|N|+|A|}$ that remains feasible, i.e., satisfies constraints (1), (2), (3) as well as all three constraints in (4), for any $\tilde{\mathbf{d}}$, $\tilde{\boldsymbol{\rho}}$, and $\tilde{\mathbf{u}}$ in the sets D, P, and U, respectively. Due to the single-stage nature of the classical robust optimization model, the post-disaster decisions $(\mathbf{x}, \mathbf{z}^+, \mathbf{z}^-)$, even though will not be implemented until the disaster attack, have to be made before the disaster along with the pre-disaster decisions $(\mathbf{y}, \mathbf{r})$ and so are independent of the realization of $(\tilde{\mathbf{d}}, \tilde{\boldsymbol{\rho}}, \tilde{\mathbf{u}})$. Now consider the first constraint in (4), which is an equality constraint with $\tilde{\mathbf{d}}$ in the right hand side. Obviously, given $\tilde{\boldsymbol{\rho}}$ and $\tilde{\mathbf{u}}$, any solution $(\mathbf{y}, \mathbf{r}, \mathbf{x}, \mathbf{z}^+, \mathbf{z}^-)$ feasible for some $\tilde{\mathbf{d}} \in D$ becomes infeasible for a different $\tilde{\mathbf{d}} \in D$. Therefore, the classical robust counterpart of our problem is infeasible as long as D is not a singleton.

To avoid infeasibility, as in the two-stage stochastic model, we consider the pre- and post-disaster decisions as the first and second stage decisions, respectively. In this case, the pre-disaster decisions $(\mathbf{y}, \mathbf{r})$ are made before the disaster, whereas the post-disaster decisions $(\mathbf{x}, \mathbf{z}^+, \mathbf{z}^-)$ can be postponed to after observing the realization of the uncertain parameters $(\tilde{\mathbf{d}}, \tilde{\boldsymbol{\rho}}, \tilde{\mathbf{u}})$. Given the first stage decisions and the uncertainty sets D, P, and U, we can obtain the optimal post-disaster decision and the minimum post-disaster cost for any realization in $\tilde{\mathbf{d}} \in D$, $\tilde{\boldsymbol{\rho}} \in P$, and $\tilde{\mathbf{u}} \in U$. In order to protect against all possible outcomes within the uncertainty sets, we target to minimize the pre-disaster cost plus the worst-case post-disaster cost among all $\tilde{\mathbf{d}} \in D$, $\tilde{\boldsymbol{\rho}} \in P$, and $\tilde{\mathbf{u}} \in U$,

which leads to the following min-max robust formulation:

$$\begin{aligned} \min_{\mathbf{y},\mathbf{r}} \quad & \sum_{i\in N} F_i y_i + \sum_{i\in N} h_i r_i + \max_{\tilde{\mathbf{d}}\in D, \tilde{\boldsymbol{\rho}}\in P, \tilde{\mathbf{u}}\in U} \mathcal{Q}(\mathbf{r}, \tilde{\mathbf{d}}, \tilde{\boldsymbol{\rho}}, \tilde{\mathbf{u}}) \\ \text{s.t.} \quad & (1), (2), (3). \end{aligned} \tag{7}$$

Similar to the two-stage stochastic model (6), although model (7) does not explicitly define second stage decision variables for each $(\tilde{\mathbf{d}}, \tilde{\boldsymbol{\rho}}, \tilde{\mathbf{u}})$, it obtains an exclusive optimal second stage solution for each $(\tilde{\mathbf{d}}, \tilde{\boldsymbol{\rho}}, \tilde{\mathbf{u}})$ through solving the corresponding instance of the optimization problem $\mathcal{Q}(\mathbf{r}, \tilde{\mathbf{d}}, \tilde{\boldsymbol{\rho}}, \tilde{\mathbf{u}})$.

3 Analysis of the Min-Max Robust Model

The practicability and computational tractability of the robust model (7) are determined by the definitions of the uncertainty sets D, P, and U. In this section, we discuss how to define the sets D, P, and U appropriately and present computationally tractable approaches to solve model (7). Furthermore, we analyze a special case that minimizes the deprivation cost. In this special case, a closed-form optimal solution can be obtained under certain conditions. This result also sheds light on how to choose the uncertainty sets.

3.1 Uncertainty Sets

In practice, the most likely value, the upper bound, and the lower bound are among the most easily available information of an uncertain parameter. Therefore, we utilize these values to construct the uncertainty sets D, P, and U. This section focuses on the uncertainty set D for the random demands. The other two sets, i.e., P and U for the proportions of usable inventories and the road link capacities, respectively, are defined in a similar manner and briefly discussed towards the end of this section.

Consider the vector $\tilde{\mathbf{d}} \geq \mathbf{0}$ of the random demands. For each uncertain demand $\tilde{d}_i$ where $i \in N$, suppose that we know the information of the lower bound d_i^L, the upper bound d_i^U, and the most likely value d_i^M. We can define the uncertainty set D as follows:

$$D = \left\{ \tilde{\mathbf{d}} \in \mathbb{R}^{|N|} \;\middle|\; \begin{array}{l} \eta_i = \begin{cases} (d_i^M - \tilde{d}_i)/(d_i^M - d_i^L), \text{ if } \tilde{d}_i \leq d_i^M \\ (\tilde{d}_i - d_i^M)/(d_i^U - d_i^M), \text{ if } \tilde{d}_i > d_i^M \end{cases} \quad \forall i \in N, \\ \tilde{d}_i \in [d_i^L, d_i^U] \;\forall i \in N, \; \sum_{i\in N} \eta_i \leq \gamma_d \end{array} \right\}. \tag{8}$$

Here, η_i for all $i \in N$ measures the deviation of $\tilde{d}_i$ from its most likely value d_i^M. The summation of η_i is upper bounded by a given parameter γ_d, which is referred to as the uncertainty budget for $\tilde{\mathbf{d}}$ and can take any value in $\{0, 1, ..., |N|\}$.[2] Obviously, the value of γ_d controls the size of the uncertainty set D. When $\gamma_d = |N|$, D is the hyperrectangle defined by d_i^L and d_i^U for all $i \in N$. It shrinks to the singleton of d_i^M for all $i \in N$ as γ_d decreases to 0. Note that the robust model (7) considers the maximum post-disaster cost among all values of $\tilde{\mathbf{d}}$ in the set D. Therefore, γ_d determines the level of conservatism of the robust model and represents the attitude of the decision maker towards the worst-case outcome. A decision maker who cares more about the worst-case outcome should choose a more conservative robust model by setting a higher γ_d and vice versa.

The following proposition shows that D defined in (8) is a polytope and we can identify a superset of its vertices.

Proposition 1 *The set D in* (8) *is a polytope and its vertices are contained in the set*

$$V_d = \bigcup_{T \subseteq N, |T| = \gamma_d} \left\{ \mathbf{d} \in \mathbb{R}^{|N|} \;\middle|\; \begin{array}{ll} d_i \in \{d_i^L, d_i^U\}, & \forall i \in T \\ d_i = d_i^M, & \forall i \in N \setminus T \end{array} \right\}. \tag{9}$$

The proof of Proposition 1 is presented in Appendix A.1. Note that V_d can be reduced to the uncertainty set in Bertsimas and Sim (2004) with an integral uncertainty budget γ_d if we set $d_i^U - d_i^M = d_i^M - d_i^L$ for any $i \in N$. As it is straightforward to allow an arbitrary $\gamma_d \in [0, |N|]$, D is as general as, if not more general than, the uncertainty set in Bertsimas and Sim (2004). Also note that Proposition 1 plays an important role in solving the robust model (7). As shown later in Section 3.2, the uncertainty set D in model (7) can be replaced by a superset of its vertices without sacrificing the robustness of model (7).

Similarly, for the proportion of usable inventory $\tilde{\rho}_i \geq 0$ and the link capacity $\tilde{u}_{ij} \geq 0$, suppose that we know the most likely values ρ_i^M and u_{ij}^M, the lower bounds ρ_i^L and u_{ij}^L, as well as the upper bounds ρ_i^U and u_{ij}^U. The uncertainty sets P and U for these two groups of random parameters can

[2] Our results can be easily generalized to the case where $\gamma_d \in [0, |N|]$. Here we restrict γ_d to be an integer because the notations are substantially simpler.

be defined as

$$P = \left\{ \tilde{\boldsymbol{\rho}} \in \mathbb{R}^{|N|} \;\middle|\; \begin{array}{ll} \eta_i = \begin{cases} (\rho_i^M - \tilde{\rho}_i)/(\rho_i^M - \rho_i^L), \ \tilde{\rho}_i \le \rho_i^M, \\ (\tilde{\rho}_i - \rho_i^M)/(\rho_i^U - \rho_i^M), \ \tilde{\rho}_i > \rho_i^M, \end{cases} & \forall i \in N, \\ \tilde{\rho}_i \in [\rho_i^L, \rho_i^U] \ \forall i \in N, \ \sum_{i \in N} \eta_i \le \gamma_\rho & \end{array} \right\} \tag{10}$$

and

$$U = \left\{ \tilde{\mathbf{u}} \in \mathbb{R}^{|A|} \;\middle|\; \begin{array}{ll} \eta_{ij} = \begin{cases} (u_{ij}^M - \tilde{u}_{ij})/(u_{ij}^M - u_{ij}^L), \ \tilde{u}_{ij} \le u_{ij}^M, \\ (\tilde{u}_{ij} - u_{ij}^M)/(u_{ij}^U - u_{ij}^M), \ \tilde{u}_{ij} > u_{ij}^M, \end{cases} & \forall (i,j) \in A, \\ \tilde{u}_i \in [u_{ij}^L, u_{ij}^U] \ \forall (i,j) \in A, \ \sum_{(i,j) \in A} \eta_{ij} \le \gamma_u & \end{array} \right\}, \tag{11}$$

where $\gamma_\rho \in \{0, 1, ..., |N|\}$ and $\gamma_u \in \{0, 1, ..., |A|\}$ are the uncertainty budgets for $\tilde{\boldsymbol{\rho}}$ and $\tilde{\mathbf{u}}$ that adjust the conservatism of the robust model. Following the proof of Proposition 1, both P and U are polytopes, and their vertices are contained in the sets

$$V_\rho = \bigcup_{T \subseteq N, |T| = \gamma_\rho} \left\{ \boldsymbol{\rho} \in \mathbb{R}^{|N|} \;\middle|\; \begin{array}{ll} \rho_i \in \{\rho_i^L, \rho_i^U\}, & \forall i \in T \\ \rho_i = \rho_i^M, & \forall i \in N \setminus T \end{array} \right\} \tag{12}$$

and

$$V_u = \bigcup_{T \subseteq A, |T| = \gamma_u} \left\{ \mathbf{u} \in \mathbb{R}^{|A|} \;\middle|\; \begin{array}{ll} u_{ij} \in \{u_{ij}^L, u_{ij}^U\}, & \forall (i,j) \in T \\ u_{ij} = u_{ij}^M, & \forall (i,j) \in A \setminus T \end{array} \right\}, \tag{13}$$

respectively.

3.2 A General Min-Max Robust Optimization Framework

In this section and the next, we present computationally tractable reformulations of the robust model (7) under the uncertainty sets D, P, and U defined in (8), (10), and (11). In particular, this section considers a generalization of model (7) and thus can be applied to any two-stage min-max robust optimization problem whose second stage constraints contain uncertainties in both the left-hand-side coefficients of the first stage decision variables and the right-hand-side coefficients. The next section then focuses on model (7) and obtains reformulations with reduced scales by applying the model-specific properties.

First, let us introduce the following problem:

$$\min_{\mathbf{x}_1} \left\{ \mathbf{c}_1^T \mathbf{x}_1 + \max_{\tilde{\mathbf{A}}_2 \in M_A, \tilde{\mathbf{b}}_2 \in M_b} \mathcal{Q}(\mathbf{x}_1, \tilde{\mathbf{A}}_2, \tilde{\mathbf{b}}_2) : \mathbf{x}_1 \in X \right\} \tag{14}$$

where

$$\mathcal{Q}(\mathbf{x}_1, \tilde{\mathbf{A}}_2, \tilde{\mathbf{b}}_2) = \min_{\mathbf{x}_2} \Big\{ \mathbf{c}_2^T \mathbf{x}_2 : (\mathbf{\Phi}\tilde{\mathbf{A}}_2 + \mathbf{\Psi})\mathbf{x}_1 + \mathbf{B}\mathbf{x}_2 = \mathbf{\Xi}\tilde{\mathbf{b}}_2 + \boldsymbol{\xi},\ \mathbf{x}_2 \geq 0 \Big\}. \tag{15}$$

Here, the first and second stage decision variables are denoted by $\mathbf{x}_1$ and $\mathbf{x}_2$, respectively. The uncertain parameters in the second stage are $\tilde{\mathbf{A}}_2$ and $\tilde{\mathbf{b}}_2$, which appear in both the left and right hand sides of the constraints in the second stage problem $\mathcal{Q}(\mathbf{x}_1, \tilde{\mathbf{A}}_2, \tilde{\mathbf{b}}_2)$. The uncertainty sets for $\tilde{\mathbf{A}}_2$ and $\tilde{\mathbf{b}}_2$ are M_A and M_b, respectively. Moreover, X is a known set defining the feasible region of $\mathbf{x}_1$ and the remaining parameters, i.e., $\mathbf{c}_1$, $\mathbf{c}_2$, $\mathbf{B}$, $\mathbf{\Phi}$, $\mathbf{\Psi}$, $\mathbf{\Xi}$, and $\boldsymbol{\xi}$, are deterministic vectors and matrices with proper sizes. Note that model (14) is well defined only if $\mathcal{Q}(\mathbf{x}_1, \tilde{\mathbf{A}}_2, \tilde{\mathbf{b}}_2)$ is (i) feasible for all $\tilde{\mathbf{A}}_2 \in M_A$ and $\tilde{\mathbf{b}}_2 \in M_b$ and (ii) bounded for some $\tilde{\mathbf{A}}_2 \in M_A$ and $\tilde{\mathbf{b}}_2 \in M_b$. Therefore, we assume that these two conditions hold in the subsequent analysis.

Model (14) is more general than most two-stage min-max robust optimization problems studied in the literature, where only right-hand-side uncertainty is considered, i.e., the matrix $\tilde{\mathbf{A}}_2$ in model (14) is assumed to be deterministic. Furthermore, it is straightforward that model (7) is a special case of model (14) and satisfies conditions (i) and (ii). The following theorem presents an equivalent formulation of model (14), which is proved in Appendix A.2.

Theorem 2 *Suppose that M_A and M_b are nonempty bounded polyhedra and $V_A \subseteq M_A$ and $V_b \subseteq M_b$ are supersets of their vertices, respectively. Model* (14) *is equivalent to*

$$\min_{\mathbf{x}_1} \left\{ \mathbf{c}_1^T \mathbf{x}_1 + \max_{\tilde{\mathbf{A}}_2 \in V_A, \tilde{\mathbf{b}}_2 \in V_b} \mathcal{Q}(\mathbf{x}_1, \tilde{\mathbf{A}}_2, \tilde{\mathbf{b}}_2) : \mathbf{x}_1 \in X \right\}. \tag{16}$$

Compared with model (14), model (16) considers the worst-case second stage cost among all realizations in V_A and V_b, instead of the original uncertainty sets M_A and M_b. In other words, we can achieve the same level of robustness by considering the supersets of the vertices of the uncertainty sets. This result is of great importance computationally. In particular, as long as V_A and V_b are finite sets, model (16) yields an equivalent compact reformulation of model (14), which can be readily solved by commercial optimization packages or Benders decomposition. In the following Section 3.3, the general result in Theorem 2, jointly with Proposition 1 that characterizes the vertices of the uncertainty sets, is applied to solve the min-max robust model (7). Some problem-specific properties are also exploited to improve the computational efficiency.

3.3 Solving Model

Obviously, our min-max robust model (7) fits into the framework (14). Applying Theorem 2, we obtain the following equivalent formulation of model (7):

$$\begin{aligned} \min_{\mathbf{y},\mathbf{r}} \quad & \sum_{i\in N} F_i y_i + \sum_{i\in N} h_i r_i + \max_{\tilde{\mathbf{d}}\in V_d, \tilde{\boldsymbol{\rho}}\in V_\rho, \tilde{\mathbf{u}}\in V_u} \mathcal{Q}(\mathbf{r}, \tilde{\mathbf{d}}, \tilde{\boldsymbol{\rho}}, \tilde{\mathbf{u}}) \\ \text{s.t.} \quad & (1), (2), (3), \end{aligned} \tag{17}$$

where $V_d \subseteq D$, $V_\rho \subseteq P$, and $V_u \subseteq U$ are supersets of the vertices of D, P, and U defined in (9), (12), and (13), respectively. Model (17) can be written in a compact form if we insert in the definition of $\mathcal{Q}(\mathbf{r}, \tilde{\mathbf{d}}, \tilde{\boldsymbol{\rho}}, \tilde{\mathbf{u}})$ in (4). The resulting formulation is a standard mixed integer program (MIP) that contains a copy of the decision variables, objective function, and constraints in $\mathcal{Q}(\mathbf{r}, \tilde{\mathbf{d}}, \tilde{\boldsymbol{\rho}}, \tilde{\mathbf{u}})$ for each $\tilde{\mathbf{d}} \in V_d$, $\tilde{\boldsymbol{\rho}} \in V_\rho$, and $\tilde{\mathbf{u}} \in V_u$. Note that $|V_d|$, $|V_\rho|$, and $|V_u|$ are all polynomial in $|N|$ and $|A|$. Thus, in the MIP formulation of model (17), the numbers of variables and constraints are both polynomial in $|N|$ and $|A|$. In the following proposition, we utilize the properties of the second stage problem $\mathcal{Q}(\mathbf{r}, \tilde{\mathbf{d}}, \tilde{\boldsymbol{\rho}}, \tilde{\mathbf{u}})$ defined in (4) and the sets V_d, V_ρ, and V_u to reduce the scale of model (17). Its proof is presented in Appendix A.3.

Proposition 3 *Let*

$$\begin{aligned} V_{(d,\rho)} &= \big\{(\mathbf{d}, \boldsymbol{\rho}) \in V_d \times V_\rho : (d_i - d_i^M)(\rho_i - \rho_i^M) \le 0, \forall i \in N\big\} \\ \bar{V}_u &= \big\{\mathbf{u} \in V_u : u_{ij} \le u_{ij}^M, \forall (i,j) \in A\big\}, \end{aligned}$$

where V_d, V_ρ, and V_u are defined in (9), (12), *and* (13), *respectively. Given D, P, and U defined in* (8), (10), *and* (11), *model* (7) *is equivalent to*

$$\begin{aligned} \min_{\mathbf{y},\mathbf{r}} \quad & \sum_{i\in N} F_i y_i + \sum_{i\in N} h_i r_i + \max_{(\tilde{\mathbf{d}}, \tilde{\boldsymbol{\rho}})\in V_{(d,\rho)}, \tilde{\mathbf{u}}\in \bar{V}_u} \mathcal{Q}(\mathbf{r}, \tilde{\mathbf{d}}, \tilde{\boldsymbol{\rho}}, \tilde{\mathbf{u}}) \\ \textit{s.t.} \quad & (1), (2), (3). \end{aligned} \tag{18}$$

Comparing models (17) and (18) reveals that we can protect against all scenarios in $V_d \times V_\rho \times V_u$ by simply considering those in $V_{(d,\rho)} \times \bar{V}_u$. Similar to model (17), model (18) can also be reformulated as a standard MIP. It has significantly smaller numbers of variables and constraints than the MIP for model (17) because $|V_{(d,\rho)}| \le |V_d| \times |V_\rho|$ and $|\bar{V}_u| \le |V_u|$. If $|V_{(d,\rho)}| \times |\bar{V}_u|$ is moderate, the MIP for model (18) can be directly solved by commercial MIP solvers, e.g., IBM ILOG CPLEX. When

$|V_{(d,\rho)}| \times |\bar{V}_u|$ is large, we can consider the following equivalent formulation of model (7) and solve it by Benders decomposition.

Proposition 4 *For any given* $\mathbf{r} \geq \mathbf{0}$*, define* $\bar{\gamma}_\rho(\mathbf{r}) = \min\left\{\gamma_\rho, |\{i \in N : r_i > 0\}|\right\}$ *and*

$$\bar{V}_\rho(\mathbf{r}) = \bigcup_{\substack{T \subseteq \{i \in N : r_i > 0\}, \\ |T| = \bar{\gamma}_\rho(\mathbf{r})}} \left\{ \boldsymbol{\rho} \in \mathbb{R}^{|N|} \;\middle|\; \begin{array}{ll} \rho_i \in \{\rho_i^L, \rho_i^U\}, & \forall i \in T \\ \rho_i = \rho_i^M, & \forall i \in N \setminus T \setminus \{t\} \end{array} \right\}.$$

Given D*,* P*, and* U *defined in* (8)*,* (10)*, and* (11)*, model* (7) *is equivalent to*

$$\begin{array}{ll} \min\limits_{\mathbf{y},\mathbf{r}} & \sum\limits_{i \in N} F_i y_i + \sum\limits_{i \in N} h_i r_i + \max\limits_{(\tilde{\mathbf{d}}, \tilde{\boldsymbol{\rho}}) \in \bar{V}_{(d,\rho)}(\mathbf{r}), \tilde{\mathbf{u}} \in \bar{V}_u} \mathcal{Q}(\mathbf{r}, \tilde{\mathbf{d}}, \tilde{\boldsymbol{\rho}}, \tilde{\mathbf{u}}) \\ s.t. & (1), (2), (3). \end{array} \tag{19}$$

where $\bar{V}_u$ *is defined in Proposition 3 and*

$$\bar{V}_{(d,\rho)}(\mathbf{r}) = \left\{(\mathbf{d}, \boldsymbol{\rho}) \in V_d \times \bar{V}_\rho(\mathbf{r}) : (d_i - d_i^M)(\rho_i - \rho_i^M) \leq 0 \ \forall i \in N\right\}.$$

The proof of Proposition 4 is presented in Appendix A.4. Model (19) further narrows down the realizations we should consider to those in $\bar{V}_{(d,\rho)}(\mathbf{r}) \times \bar{V}_u$. Unfortunately, it is rather difficult to reformulate model (19) as a compact MIP because of the nonlinear dependence of $\bar{V}_{(d,\rho)}(\mathbf{r})$ on $\mathbf{r}$. Nevertheless, it is straightforward to develop an algorithm for model (19) based on Bender decomposition. Note that Bender decomposition can also be applied to solve model (18), but it is more efficient to solve model (19) because $|\bar{V}_{(d,\rho)}(\mathbf{r})| \leq |V_{(d,\rho)}|$, especially when the fixed costs to set up facilities are not negligible.

3.4 Minimizing the Deprivation Cost

The premier objective of all disaster response operations should be to minimize human suffering, which can be measured by the deprivation cost introduced in Holguín-Veras et al. (2013). For this purpose, this section studies a deprivation cost minimization version of model (7).

Holguín-Veras et al. (2013) consider deprivation cost as "the economic valuation of the human suffering associated with a lack of access to a good or service". It obviously depends on the deprivation time, i.e., how long the good or service has been unavailable. For a given individual, the

deprivation cost function, representing how the deprivation cost changes with respect to the deprivation time, should be increasing, non-linear, and convex. The deprivation cost should also vary according to the socioeconomic characteristics of individuals. However, as the detailed data about the suffering population is often lacked, a generic deprivation cost function, i.e., one independent of the socioeconomic characteristics, might be the best alternative. Holguín-Veras et al. (2016) then propose a process to estimate deprivation cost functions using contingent valuation.

In this paper, we focus on the deprivation cost for the emergence supplies considered in the single-commodity network. Some individuals in the affected areas could get the supplies from the pre-positioned inventories. For these individuals, the deprivation time is rather short and so the deprivation cost is very close to zero (cf. Holguín-Veras et al., 2013). Therefore, the deprivation cost for these individuals is set to zero. In other words, for each unit of demand satisfied by the propositioned inventories, the associated deprivation cost is zero. Note that this assumption can be easily relaxed.

For the individuals whose demands cannot be satisfied by the pre-positioned inventories, they have to be served by deliveries from the unaffected areas in the post-disaster operations. Suppose that it takes T time units for these individuals to get the supply, where T can be determined in the pre-disaster stage based on the geographic location of the nodes. Then the deprivation time for this group of individuals is T. Given the generic deprivation cost function denoted by $\mathrm{DCF}(t)$, which can be estimated using the approach designed in Holguín-Veras et al. (2016), the deprivation cost for each of these individuals is $\mathrm{DCF}(T)$. Let n denote the number of individuals that can be served by one unit of the emergency supplies. For each unit of shortage, i.e., each unit of demand that cannot be satisfied using the pre-positioned inventories, the corresponding deprivation cost is $\mathrm{DCF}(T) \cdot n$.

Under this setting, model (7) obviously minimizes the total deprivation cost if we let q_i^- be the deprivation cost for each unit of shortage, i.e., $q_i^- = \mathrm{DCF}(T) \cdot n$, for all $i \in N$ and ignore other cost components, which are merely economic costs. We can also remove all the restrictions on the disaster relief network $\mathcal{G}(N, A)$ so that the network is strongly connected with no capacity limits on both nodes and links. Without economic considerations, this can be easily justified as the capacity of each open facility could be sufficiently large and the pre-positioned inventories, if usable, can be quickly sent to any place in need via helicopters. Along with other conditions, the

following theorem, whose proof is presented in Appendix A.5, provides a closed-form solution for the problem that minimizes the deprivation cost.

Theorem 5 *Suppose that (i) $\mathcal{G}(N, A)$ is strongly connected and uncapacitated, (ii) $F_i = h_i = q_i^+ = 0$ for all $i \in N$, and (iii) $c_{ij} = 0$ for all $(i, j) \in A$. Consider model (7) with D and P defined in (8) and (10), respectively. An optimal solution $(\mathbf{y}^*, \mathbf{r}^*)$ with $y_i^* = 1$ for all $i \in N$ is characterized for the following cases.*

(a) If $\gamma_\rho = 0$, $r_{i^*}^* = R$ for some $i^* \in \arg\max\{\rho_i^M : i \in N\}$ and $r_i^* = 0$ for all $i \in N \setminus \{i^*\}$.

(b) If $\gamma_\rho = |N|$, $r_{i^*}^* = R$ for some $i^* \in \arg\max\{\rho_i^L : i \in N\}$ and $r_i^* = 0$ for all $i \in N \setminus \{i^*\}$.

(c) Suppose that $\rho_i^M = \rho_i^L + \delta$ for all $i \in N$ and, WLOG, $\rho_1^M \geq \rho_2^M \geq \cdots \geq \rho_{|N|}^M$. If $\gamma_\rho \in \{1, ..., |N|-1\}$, then $r_i^* = R/n_{\gamma_\rho}^*$ for all $i \in \{1, ..., n_{\gamma_\rho}^*\}$ and $r_i^* = 0$ for all $i \in \{n_{\gamma_\rho}^* + 1, ..., |N|\}$, where

$$n_{\gamma_\rho}^* \in \arg \max_{i \in \{1,...,|N|\}} \left\{ \frac{1}{i} \left(\sum_{j=1}^{i} \rho_j^M - \min\{i, \gamma_\rho\}\delta \right) \right\}.$$

(d) Suppose that $\rho_i^M = \rho^M$ for all $i \in N$ and, WLOG, $\rho_1^L \geq \rho_2^L \geq \cdots \geq \rho_{|N|}^L$. If $\gamma_\rho \in \{1, ..., |N| - 1\}$, then

$$r_i^* = R \cdot \frac{(\rho^M - \rho_i^L)^{-1}}{\sum_{j=1}^{n_{\gamma_\rho}^*} (\rho^M - \rho_i^L)^{-1}}$$

for all $i \in \{1, ..., n_{\gamma_\rho}^*\}$ and $r_i^* = 0$ for all $i \in \{n_{\gamma_\rho}^* + 1, ..., |N|\}$, where

$$n_{\gamma_\rho}^* \in \arg \min_{i \in \{1,...,|N|\}} \left\{ \frac{\min\{i, \gamma_\rho\}}{\sum_{j=1}^{i} (\rho^M - \rho_j^L)^{-1}} \right\}.$$

(e) Suppose that $\rho_i^L = \rho^L$ for all $i \in N$ and, WLOG, $\rho_1^M \geq \rho_2^M \geq \cdots \geq \rho_{|N|}^M$. If $\gamma_\rho \in \{1, ..., |N| - 1\}$, then

$$r_i^* = R \cdot \frac{(\rho_i^M - \rho^L)^{-1}}{\sum_{j=1}^{n_{\gamma_\rho}^*} (\rho_i^M - \rho^L)^{-1}}$$

for all $i \in \{1, ..., n_{\gamma_\rho}^*\}$ and $r_i^* = 0$ for all $i \in \{n_{\gamma_\rho}^* + 1, ..., |N|\}$, where

$$n_{\gamma_\rho}^* \in \arg \max_{i \in \{1,...,|N|\}} \left\{ \frac{(i - \gamma_\rho)^+}{\sum_{j=1}^{i} (\rho_j^M - \rho^L)^{-1}} \right\}.$$

In Theorem 5 (a), the uncertainty budget γ_ρ for $\tilde{\boldsymbol{\rho}}$, which controls the conservatism of the robust model, is set to 0. The robust model with $\gamma_\rho = 0$ is the least conservative and equivalent to the deterministic model where the proportions of usable inventories are set to ρ_i^M for all $i \in N$. Its optimal solution puts all inventories in the location with the highest ρ_i^M. Theorem 5 (b) then considers the model with $\gamma_\rho = |N|$, which is the most conservative and protects against all realizations in the hyperrectangle defined by ρ_i^L and ρ_i^U for all i. The optimal solution then puts all inventories in the location with the highest ρ_i^L. These results suggest that we will only use one location as long as $\gamma_d \in \{0, |N|\}$, which could be risky as all eggs are put in one basket. Therefore, a more desirable solution should utilize more locations to reduce the risk. Theorem 5 (c), (d), and (e) then consider $\gamma_\rho \in \{1, ..., |N|-1\}$. These three parts correspond to the cases that the differences between ρ_i^M and ρ_i^L, the most likely values ρ_i^M, and the lower bounds ρ_i^L are the same for all nodes, respectively. The results indicate that the corresponding solution pre-positions inventories in $n^*_{\gamma_\rho}$ locations. The following proposition reveals some insights on when $n^*_{\gamma_\rho} = 1$ for different γ_ρ.

Proposition 6 *(c,d) Consider $n^*_{\gamma_\rho}$ defined in Theorem 5 (c) or (d). For any $\gamma_\rho, \gamma'_\rho \in \{1, ..., |N|-1\}$ such that $\gamma_\rho \leq \gamma'_\rho$, if $n^*_{\gamma_\rho} = 1$ is the unique optimal solution to the optimization problem defining $n^*_{\gamma_\rho}$, then $n^*_{\gamma'_\rho} = 1$ is the unique optimal solution to the optimization problem defining $n^*_{\gamma'_\rho}$.*

(e) Consider $n^*_{\gamma_\rho}$ defined in Theorem 5 (e). $n^*_{\gamma_\rho} > 1$ for any $\gamma_\rho \in \{1, ..., |N| - 1\}$.

The proof of Proposition 6 is shown in Appendix A.6. For the cases in Theorem 5 (c) and (d), Proposition 6 shows that if the robust model with an uncertainty budget in $\{1, ..., |N|-1\}$ only uses one location, then any robust model whose uncertainty budget is higher should also use exactly one location. Furthermore, the robust model with any uncertainty budget γ_ρ in $\{1, ..., |N| - 1\}$ uses at least two locations as long as the condition in Theorem 5 (e) is satisfied. As a result, under the conditions in Theorem 5 (c), (d), and (e), the robust model with $\gamma_\rho = 1$ is most likely to use more than one location. Note that these conditions can easily hold in real circumstances. Typically, it could be difficult to estimate the variation of ρ_i, i.e., $\rho_i^M - \rho_i^L$, for each $i \in N$. A practical approach is to set $\rho_i^M - \rho_i^L = \delta$ for all $i \in N$, which corresponds to the condition in Theorem 5 (c). This observation suggests that the robust model with $\gamma_\rho = 1$ may yield a more desirable solution than those obtained from models with other values of γ_ρ.

Furthermore, in most cases, a disaster, e.g., an earthquake, has an epicenter. In the disaster relief network, the node/link closest to the epicenter may suffer the most from the disaster, while

the others may suffer less. Therefore, for the uncertain parameters, e.g., the demands $\tilde{d}_i$ for all $i \in N$, it is highly possible that the realization of $\tilde{d}_{i^*}$ for some $i^* \in N$ is very close to the upper bound $d^U_{i^*}$, whereas the others are close to the most likely values d^M_i for all $i \in N \setminus \{i^*\}$. Such a scenario corresponds to an extreme point of an uncertainty set whose uncertainty budget equals one. Concurring with Proposition 6, this observation also suggests setting the uncertainty budgets to ones in the disaster relief robust model (7).

4 Case Study

In this section, we use the earthquake that happened at Yushu County in Qinghai Province, PR China in the year of 2010 as the case to evaluate the performances of the deterministic, two-stage stochastic, and min-max robust models outlined in Section 2. This M_S7.1 earthquake caused massive-scale social and economic damages. Its affected area is shown in Figure 1.[3] We first consider the models with uncapacitated road links and then move on to the models with capacitated road links and additional helicopter links. All numerical experiments in this paper are conducted on a Dell desktop with 3.20GHz Intel i7 CPU and 16G memory running the Windows 7 Professional 64bit operating system. In addition, the robust models are all solved by Benders decomposition.

4.1 Uncapacitated Instances

The network in the affected area consists of 13 nodes and 15 road links (cf. Figure 2). We temporarily assume all the road links have unlimited transportation capacity. The capacitated models with a set of helicopter links are studied in Section 4.2. The input parameters are estimated to closely represent the real situation, but should be served for illustrative purpose only. Please refer to Appendix B for how the inputs are obtained. Figure 2 gives the per unit transportation cost for each road link and the other cost parameters, i.e., F_i, h_i, q^+_i and q^-_i for all $i \in N$, are listed in Table 4.

We use $N(\mu, \sigma, a, b)$ to denote a truncated normal distribution where μ and σ correspond to the mean and standard deviation of the "parent" normal distribution and (a, b) specifies the truncation interval. For any $i \in N$, the post-disaster demand $\tilde{d}_i$ and the usable portion of the pre-positioned

[3]Source: http://image.dili360.com/www/201004/yutian_liedu.jpg

Figure 1: The affected area

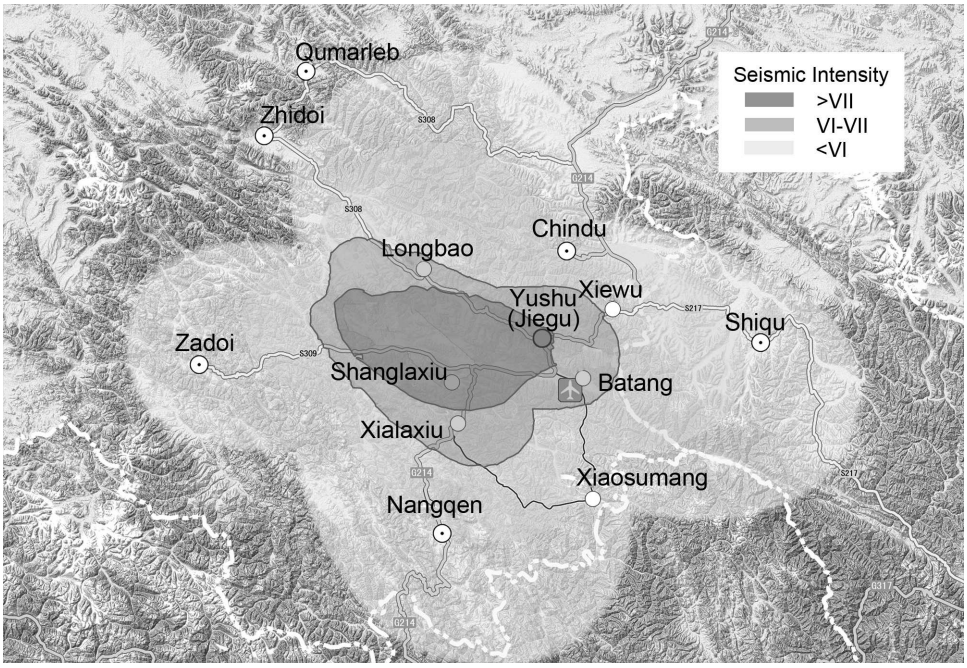

inventory $\tilde{\rho}_i$ are assumed to follow independent truncated normal distributions $N(\mu_i^d, \sigma_i^d, 0, +\infty)$ and $N(\mu_i^\rho, \sigma_i^\rho, 0, 1)$, respectively. As in practice, these distributions are unknown to the decision makers. The only available information is the forecasted most likely values, upper bounds, and lower bounds of the uncertain parameters, i.e., $(d_i^M, d_i^L, d_i^U; \rho_i^M, \rho_i^L, \rho_i^U)$ for all $i \in N$. We refer to a set of parameters $(d_i^M, d_i^L, d_i^U; \rho_i^M, \rho_i^L, \rho_i^U)$ for all $i \in N$ as an instance. To generate an instance, we let d_i^M, d_i^L, and d_i^U be the average, minimum, and maximum of 50 independent samples drawn from $N(\mu_i^d, \sigma_i^d, 0, +\infty)$, respectively. Similarly, ρ_i^M, ρ_i^L, and ρ_i^U are set to the average, minimum, and maximum of 50 independent samples drawn from $N(\hat{\mu}_i^\rho, \sigma_i^\rho, 0, 1)$.

In this experiment, we generate 50 instances with $\mu_i^d = 100$, $\sigma_i^d = 10$, μ_i^ρ and $\hat{\mu}_i^\rho$ shown in Table 4, and $\sigma_i^\rho = 0.1$ for all $i \in N$. The capacity M_i of any node $i \in N$ is set to 800. The total supply R could be any value in the set $\{2300, 2400, ..., 3000\}$. For each instance and possible R, we compare the deterministic model (5), the two-stage stochastic model (6), and the min-max robust models (7) using the following procedure.

Step 1. The deterministic, stochastic, and robust models are constructed as follows.

- The deterministic model is obtained by replacing $\mathbf{d}$ and $\boldsymbol{\rho}$ in model (5) with d_i^M and ρ_i^M

Figure 2: Disaster relief network

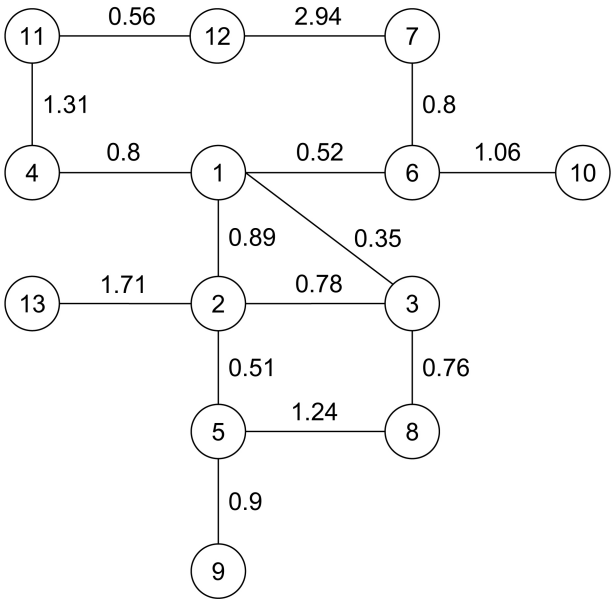

for all $i \in N$.

- For the two-stage stochastic model (6), we consider 100 scenarios, i.e., $|S| = 100$. Each scenario $s \in S$ consists of independent samples drawn from triangular distributions $T(d_i^L, d_i^M, d_i^U)$ and $T(\rho_i^L, \rho_i^M, \rho_i^U)$ for all $i \in N$, which corresponds to $\tilde{d}_i$ and $\tilde{\rho}_i$, respectively. Here, $T(a, b, c)$ denotes a triangular distribution with lower limit a, mode b, and upper limit c.
- In the min-max robust model (7), the uncertainty sets D and P are defined using $(d_i^M, d_i^L, d_i^U; \rho_i^M, \rho_i^L, \rho_i^U)$ as in (8) and (10). Furthermore, we consider three different levels of conservatism by simultaneously setting the uncertainty budgets γ_d and γ_ρ to 1, 2, and $|N|$, respectively.

We solve all the above models to optimality and obtain the optimal first stage solution, i.e., the location and pre-positioning decisions $(\mathbf{y}, \mathbf{r})$, for each of these models.

Step 2. We generate 10,000 realizations of $\tilde{d}_i$ and $\tilde{\rho}_i$ using independent truncated normal distributions $N(\mu_i^d, \sigma_i^d, 0, +\infty)$ and $N(\mu_i^\rho, \sigma_i^\rho, 0, 1)$, respectively. For each of the first stage solutions obtained in Step 1 and each of the realizations, we solve the corresponding second stage

Table 4: Input parameters for each node

Node	1	2	3	4	5	6	7	8	9	10	11	12	13
F_i	203	193	130	117	292	174	130	157	134	161	234	220	170
h_i	3.40	2.33	2.00	2.69	2.63	3.44	3.43	3.53	2.33	2.50	3.37	2.84	3.76
q_i^+	2.81	2.58	2.86	2.42	3.28	3.05	2.77	2.68	2.52	3.14	2.93	2.85	2.87
q_i^-	11.48	14.32	12.14	16.19	12.01	14.90	9.42	11.91	10.68	11.24	13.1	11.09	10.18
μ_i^ρ	0.05	0.05	0.20	0.18	0.18	0.72	0.76	0.70	0.60	0.70	0.78	0.62	0.68
$\hat{\mu}_i^\rho$	0.46	0.49	0.51	0.45	0.46	0.52	0.55	0.51	0.44	0.51	0.57	0.45	0.49

problem (4) and compute the cost of both the first and second stages for this realization.

Step 3. For each model constructed in Step 1, using the corresponding costs for the 10,000 realizations obtained in Step 2, we calculate the average and the 95% percentile of these costs, which are denoted by $\bar{C}^D$ and $C^D_{95\%}$ for the deterministic model, $\bar{C}^S$ and $C^S_{95\%}$ for the stochastic model, and $\bar{C}^R(\gamma)$ and $C^R_{95\%}(\gamma)$ for the robust model with $\gamma_d = \gamma_\rho = \gamma \in \{1, 2, |N|\}$, respectively. Note that the average cost and the 95% percentile are estimators of the expectation and the 5% value-at-risk of the cost associated with implementing the corresponding first stage solution under the true distribution of the uncertain parameters. The improvements of the robust model with respect to the deterministic and stochastic models in the average cost are then computed by $1-\bar{C}^R(\gamma)/\bar{C}^D$ and $1-\bar{C}^R(\gamma)/\bar{C}^S$ for each $\gamma \in \{1, 2, |N|\}$, respectively. Similarly, the improvements in the 95% percentile correspond to $1 - C^R_{95\%}(\gamma)/C_{95\%}$ and $1 - C^R_{95\%}(\gamma)/C^S_{95\%}$ for each $\gamma \in \{1, 2, |N|\}$, respectively.

For all the 50 instances, the robust models in Step 1 can be solved efficiently. The average computational times to solve models with uncertainty budgets 1, 2, and $|N|$ are 1, 86, and 89 seconds, respectively. Table 5 presents the average improvements of the 50 instances in both the average cost (cf. columns titled "Avg.") and the 95% percentile (cf. columns titled "95%") for different values of supply R.

Table 5 demonstrates that the min-max robust model outperforms both the deterministic and two-stage stochastic models for all uncertain budgets 1, 2, and $|N|$. For instance, when the uncertainty budgets γ_d and γ_ρ are set to 1, the average cost and 95% percentile of the robust model are

13.96% and 15.39% lower than those of the stochastic model, respectively. When comparing with the deterministic model, the improvements are more significant, reaching 18.58% and 19.47% in the average cost and 95% percentile, respectively. Note that the improvements of the robust model with respect to the deterministic model are higher than those with respect to the stochastic model. This observation suggests that the stochastic model performs better than the deterministic model. It is expected because the deterministic model completely ignores the uncertainties in the inputs, whereas the stochastic model takes them into account. We also observe that the robust model has better improvements in the 95% percentile than the average cost. Recall that the min-max robust model considers the worst-case cost among all possible realizations falling in the uncertainty set. Intuitively, compared with the average cost, the 95% percentile should be closer to the worst-case cost, which explains this observation. Furthermore, Table 5 shows that the least conservative robust model, i.e., the one with $\gamma_d = \gamma_\rho = 1$, has the best performance, which agrees with the insight from Section 3.4. Actually, the improvements in both the average cost and 95% percentile tend to be smaller with greater uncertainty budgets, implying that the more conservative robust models may sacrifice too much in the attempt to protect the worst case.

Table 5: Improvements of the robust model vs. the deterministic and stochastic models

R	Robust vs. Deterministic (%)						Robust vs. Stochastic (%)					
	$\gamma_d, \gamma_\rho = 1$		$\gamma_d, \gamma_\rho = 2$		$\gamma_d, \gamma_\rho = \lvert N \rvert$		$\gamma_d, \gamma_\rho = 1$		$\gamma_d, \gamma_\rho = 2$		$\gamma_d, \gamma_\rho = \lvert N \rvert$	
	Avg.	95%	Avg.	95%	Avg.	95%	Avg.	95%	Avg.	95%	Avg.	95%
2300	16.06	16.16	13.10	14.49	5.33	5.65	14.01	14.41	11.03	12.76	3.35	4.01
2400	17.66	18.04	13.08	14.73	5.06	5.96	14.59	15.12	9.89	11.75	2.54	3.76
2500	15.19	16.37	10.04	12.31	4.23	6.32	13.67	14.91	8.48	10.82	2.60	4.88
2600	15.90	17.97	10.50	13.23	5.21	8.32	14.88	17.00	9.46	12.26	4.00	7.18
2700	18.47	20.83	13.75	16.50	10.79	12.81	14.69	17.48	9.78	13.03	5.74	8.31
2800	24.03	24.80	21.85	24.25	17.26	18.75	12.26	14.61	9.55	13.83	5.93	8.90
2900	22.09	22.32	19.44	22.02	14.90	17.50	14.14	15.36	11.04	14.88	7.11	10.71
3000	19.23	19.28	17.08	19.02	11.78	15.88	13.46	14.21	11.02	13.84	5.49	10.60

To shed light on why the robust model performs better, for any given R, we focus on the instance where the robust model with $\gamma_d = \gamma_\rho = 1$ achieves the maximum improvement in the

average cost with respect to the stochastic model. The corresponding inventory pre-positioning decisions of the stochastic and robust models are shown in Table 6, where each row corresponds to such an instance. Table 7 then displays the average costs for each cost component under the stochastic and robust solutions, which are computed based on the 10,000 realization generated in Step 2. The columns titled "F", "h", "c", "q^+", and "q^-" represent the fixed cost, the commodity handling cost, the transportation cost, the penalty cost for unused inventory, and the penalty cost for unsatisfied demand, respectively. The column titled "Improv." shows the improvement of the robust model with respect to the stochastic model in the average cost for each instance.

Table 6: Inventory pre-positioning decisions of the stochastic and robust models

Model	Stochastic						Robust ($\gamma_d, \gamma_\rho = 1$)						
Node	2	3	4	9	10	11	2	3	4	9	10	11	12
$R = 2300$	799	800			324	377	393	341		489	525	551	
$R = 2400$	800	800			397	403	423	365		501	574	537	
$R = 2500$	586	800	560	266	289		450	664		411	461	514	
$R = 2600$	800	800	626		374		711	481		234	659	515	
$R = 2700$	699	800	583	287	330		606	463		459	663	509	
$R = 2800$	792	800	633	298	277		520	464		621	659	535	
$R = 2900$	786	800	655	411	248		502	509	266	681	583	358	
$R = 3000$	796	800	711	356	336		673	742		548	572		465

Table 6 suggests that the number of facilities set up by the robust model is always greater than or equal to that by the stochastic model. Furthermore, the pre-propositioned inventories of the robust model are more evenly distributed among all open facilities. For example, in the instance that maximizes the improvement when $R = 2500$, both the stochastic and robust models open 5 facilities. For the stochastic model, the inventories pre-positioned in the open facilities vary from 266 to 800, whereas the amount of inventory the robust model puts in each open facility is within the range from 411 to 664.

As the robust model sets up more facilities, it incurs higher fixed costs than the stochastic model, which is demonstrated in Table 7. Moreover, since the supplies are more evenly pre-

Table 7: Cost comparison of the stochastic and robust models

Model	Stochastic					Robust ($\gamma_d, \gamma_\rho = 1$)					
Cost	F	h	c	q^+	q^-	F	h	c	q^+	q^-	Improv.
$R = 2300$	718	5542	817	0	5613	852	5909	1259	23	1183	27.30%
$R = 2400$	718	5814	847	0	4931	852	6128	1302	46	902	25.02%
$R = 2500$	735	5812	730	0	6399	852	6219	1070	11	1649	28.33%
$R = 2600$	601	6083	731	0	7258	852	6548	1259	16	1540	30.39%
$R = 2700$	735	6293	728	0	5867	852	6780	1323	103	622	28.95%
$R = 2800$	735	6535	708	0	5996	852	7039	1387	292	192	30.14%
$R = 2900$	735	6771	694	0	5484	969	7156	1182	111	570	27.01%
$R = 3000$	735	7039	723	0	5097	838	7079	1126	57	1050	25.33%

positioned among all facilities, it is unavoidable to put a considerable amount in a facility with a relatively high commodity handling cost. Consequently, the commodity handling costs of the robust model are also higher. Nevertheless, due to more diversified pre-positioning decisions, it is very likely that a greater portion of the pre-positioned inventories would survive a disaster. This explains why the robust model has higher transportation costs and penalty costs for unused inventory, but substantially lower penalty costs for unsatisfied demand. In particular, the penalty costs for unused inventory of the robust model are positive, implying that for certain realizations, the amount of usable inventories exceeds the total demand in post-disaster relief operations. In contrast, the stochastic model has no penalty cost for unused inventory, i.e., shortage occurs in every realization. Also note that for all the instances shown in Table 7, the penalty costs of unsatisfied demand for the robust model are at most 25.78% of those for the stochastic model. This saving is so significant that even though the robust model has higher costs in all other cost components, it achieves improvements of at least 25.20% in comparison with the stochastic model.

4.2 Capacitated Instances with Helicopter Links

In the disaster relief network shown in Figure 2, all the road links are assumed to have unlimited capacities. This ignores that the actual road link capacity can be significantly affected by a disaster.

To capture this uncertainty, the capacity of each road link $(i,j) \in A$ is assumed to follow a truncated normal distribution $N(\mu_{ij}^u, \sigma_{ij}^u, 0, +\infty)$. Similar to the demands, the forecasted most likely value, lower bound, and upper bound for any $(i,j) \in A$, i.e., u_{ij}^M, u_{ij}^L, and u_{ij}^U, are generated by taking the average, minimum, and maximum of 50 independent samples drawn from the distribution $N(\mu_{ij}^u, \sigma_{ij}^u, 0, +\infty)$. This experiment considers $\mu_{ij}^u = 300$ and $\sigma_{ij}^u = 30$ for any $(i,j) \in A$.

In this context, we further assume that the emergency inventory can be delivered by helicopters via helicopter links, each of which has an unlimited capacity. This is incorporated in the network by creating additional helicopter links connecting the nodes 3 and 10, 4 and 13, and 8 and 9. The per unit transportation cost for each of the helicopter links is set to 10.

The procedure outlined in Section 4.1 can be straightforwardly generalized to this experiment. The differences are highlighted below. Due to the incorporation of the capacity parameters, each instance consists of $(d_i^M, d_i^L, d_i^U; \rho_i^M, \rho_i^L, \rho_i^U)$ for all $i \in N$ and $(u_{ij}^M, u_{ij}^L, u_{ij}^U)$ for all $(i,j) \in A$. In Step 1, the deterministic model use u_{ij}^M for all $(i,j) \in A$ to replace $\mathbf{u}$ in the objective function of model (5). When constructing the two-stage stochastic model, each scenario also contains independent samples drawn from triangle distributions $T(u_{ij}^L, u_{ij}^M, u_{ij}^U)$ representing the uncertain capacities for all $(i,j) \in A$. In the min-max robust model, we use $(u_{ij}^M, u_{ij}^L, u_{ij}^U)$ for all $(i,j) \in A$ to obtain the uncertainty set U defined in (11). The uncertainty budgets are set to (i) $\gamma_d = \gamma_\rho = \gamma_u = 1$, (ii) $\gamma_d = \gamma_\rho = \gamma_u = 2$, and (iii) $\gamma_d = \gamma_\rho = |N|$ and $\gamma_u = |A|$, respectively. Furthermore, for each of the realizations in Step 2, besides the demands and proportions of usable inventories, a sample of the uncertain capacity for each road link $(i,j) \in A$ is generated independently following the distribution $N(\mu_{ij}^u, \sigma_{ij}^u, 0, +\infty)$.

All the robust models can be solved within reasonable times. The average computational times are 1, 1009, and 83 seconds for the models with $\gamma_d = \gamma_\rho = \gamma_u = 1$, $\gamma_d = \gamma_\rho = \gamma_u = 2$, and $\gamma_d = \gamma_\rho = |N|$ and $\gamma_u = |A|$, respectively. The average improvements of the 50 instances are reported in Table 8. The observations from Table 8 are consistent with those from Table 5. The stochastic model outperforms the deterministic model, while all three robust models outperform the stochastic model. The robust models achieve greater improvements in the 95% percentile than the average cost. Furthermore, the robust model with $\gamma_d = \gamma_\rho = \gamma_u = 1$ performs better than the other two robust models, which are more conservative.

As in Section 4.1, for any given R, we also identify the instance that maximizes the improvement

Table 8: Improvements of the robust model vs. the deterministic and stochastic models for capacitated instances with helicopter links

R	Robust vs. Deterministic (%)						Robust vs. Stochastic (%)					
	$\gamma_d, \gamma_\rho, \gamma_u = 1$		$\gamma_d, \gamma_\rho, \gamma_u = 2$		$\gamma_d, \gamma_\rho = \lvert N \rvert$ and $\gamma_u = \lvert A \rvert$		$\gamma_d, \gamma_\rho, \gamma_u = 1$		$\gamma_d, \gamma_\rho, \gamma_u = 2$		$\gamma_d, \gamma_\rho = \lvert N \rvert$ and $\gamma_u = \lvert A \rvert$	
	Avg.	95%	Avg.	95%	Avg.	95%	Avg.	95%	Avg.	95%	Avg.	95%
2300	16.44	17.38	12.57	14.11	9.05	11.13	10.20	11.71	6.39	8.49	3.13	5.82
2400	18.41	19.34	12.50	14.45	6.31	9.30	13.90	15.18	7.86	10.21	1.64	5.15
2500	16.79	18.19	8.84	10.99	4.72	7.34	16.12	17.90	8.14	10.71	4.09	7.11
2600	16.88	18.76	8.98	11.40	4.60	7.73	14.17	16.91	6.00	9.38	1.58	5.69
2700	17.50	20.70	12.09	15.63	6.52	10.24	16.07	19.80	9.97	14.24	4.83	9.10
2800	25.30	26.95	21.94	25.66	16.43	19.10	15.77	18.74	11.55	17.02	5.77	10.04
2900	21.10	22.45	18.94	22.26	13.19	16.75	12.50	15.01	10.01	14.83	3.92	8.93
3000	19.66	20.94	16.71	19.04	9.72	14.25	13.65	15.80	10.33	13.75	2.83	8.55

of the robust model with $\gamma_d = \gamma_\rho = \gamma_u = 1$ in the average cost when comparing with the stochastic model. Tables 9 and 10 present the corresponding pre-positioning decisions and costs for the stochastic model and the robust model with $\gamma_d = \gamma_\rho = \gamma_u = 1$. Again, these results confirm what we observe from the uncapacitated instances. The robust model utilizes more facilities and tends to distribute the pre-positioned supplies more evenly among all open facilities. As a result, the first stage costs, i.e., the fixed and commodity handling costs, are higher. In the meantime, such pre-positioning decisions may lead to more usable inventories in post-disaster operations. Therefore, the robust model incurs higher transportation costs and penalty costs for unused inventory, but much lower penalty costs for unsatisfied demand. The reduction in penalty costs for unsatisfied demand is very substantial, which compensates the increases in other cost components and yields at least 23.30% improvements with respect to the stochastic model.

Table 9: Inventory pre-positioning decisions of the stochastic and robust models for capacitated instances with helicopter links

Model	Stochastic						Robust ($\gamma_d, \gamma_\rho, \gamma_u = 1$)						
Node	2	3	4	9	10	11	2	3	4	9	10	11	12
$R = 2300$	759	800			329	412	346	419		465	489	580	
$R = 2400$	800	800			429	371	430	380		491	563	535	
$R = 2500$	800	800	592		308		693	366		234	653	554	
$R = 2600$	800	800	643		357		701	370		310	664	554	
$R = 2700$	800	800	687		413		711	375		396	664	554	
$R = 2800$	661	800	660	341	338		527	471		630	637	535	
$R = 2900$	717	800	681	424	277		394	712	224	561	578		431
$R = 3000$	778	800	670	499	252		502	708		771	588		431

Table 10: Cost comparison of the stochastic and robust models for capacitated instances with helicopter links

Model	Stochastic					Robust ($\gamma_d, \gamma_\rho, \gamma_u = 1$)					
Cost	F	h	c	q^+	q^-	F	h	c	q^+	q^-	Improv.
$R = 2300$	718	5579	814	0	5367	852	5908	1292	21	1224	25.49%
$R = 2400$	718	5787	832	0	4979	852	6119	1423	40	985	23.52%
$R = 2500$	601	5826	685	0	7795	852	6392	1825	16	1519	28.87%
$R = 2600$	601	6086	702	0	7366	852	6625	1850	43	1061	29.30%
$R = 2700$	601	6345	725	0	6907	852	6857	1791	93	695	29.43%
$R = 2800$	735	6555	709	0	5386	852	7034	1560	280	214	25.74%
$R = 2900$	735	6785	691	0	5223	955	6921	1296	58	986	23.95%
$R = 3000$	735	7010	712	0	4927	838	7076	1722	177	453	23.30%

5 Experiment Variants

In this section, we conduct further computational experiments to study the performance of the min-max robust model on randomly generated networks with larger scales. For each instance considered in this study, we first generate the required inputs using the procedure described in the next three paragraphs and then apply the approach presented in Section 4 to compute the improvements achieved by the robust model.

For an instance with $|N|$ nodes, we first uniformly generate the nodes in a 10×10 square and label them from 1 to $|N|$. A spanning tree can be constructed by connecting i and j for any $i \in N \setminus \{1\}$ and some j randomly selected from the set $\{1, ..., i-1\}$. We then generate $0.2|N| + 1$ pairs of nodes and add the corresponding undirected arcs to the network. Note that the resulting network contains $1.2|N|$ undirected arcs, i.e., its average degree is 2.4, which is in accordance with a typical road network, e.g., the one in Figure 1.

The total amount of the emergency supplies R and the capacity M_i for each node $i \in N$ are uniformly generated in the intervals $(0.9{\cdot}200|N|, 1.1{\cdot}200|N|)$ and $(0.9{\cdot}60|N|, 1.1{\cdot}60|N|)$, respectively. The cost parameters for each node $i \in N$, i.e., F_i, h_i, q_i^+, and q_i^-, are also uniformly generated in the intervals $(10|N|, 20|N|)$, $(2, 4)$, $(2, 4)$, and $(10, 20)$, respectively. For any arc $(i, j) \in A$, the per unit transportation cost c_{ij} is proportional to the Euclidean distance between nodes i and j. They are normalized so that their average is equal to 1.

The uncertain parameters, similar to Section 4, are characterized by μ_i^d, σ_i^d, μ_i^ρ, $\hat{\mu}_i^\rho$, σ_i^ρ, μ_{ij}^u, and σ_{ij}^u for all $i \in N$ and $(i, j) \in A$. Here we let $\mu_i^d = 100$, $\sigma_i^d = 10$, $\hat{\mu}_i^\rho$ uniformly generated in $(0.45, 0.55)$, $\sigma_i^\rho = 0.1$, μ_{ij}^u uniformly generated in $(20|N|, 25|N|)$, and σ_{ij}^u uniformly generated in $(2|N|, 2.5|N|)$. Motivated by the case study of the 2010 Yushu earthquake, we randomly pick a node $i^* \in N$ as the epicenter and determine μ_i^ρ for all $i \in N$ based on $\hat{\mu}_i^\rho$ and its distance to i^*. More specifically, $\mu_i^\rho = 0.1\hat{\mu}_i^\rho$ for the 15% of the nodes that are closest to i^*, $\mu_i^\rho = 0.4\hat{\mu}_i^\rho$ for the next 25% of the nodes, and $\mu_i^\rho = 1.4\hat{\mu}_i^\rho$ for the remaining nodes.

Following the procedure presented in Section 4, we conduct the computational experiments with $|N| \in \{40, 60, ..., 100\}$ for both uncapacitated and capacitated models. The uncertainty budgets for the robust model are set to $\gamma_d = \gamma_\rho = \gamma_u = 1$, which yield the best performance in the case study in Section 4. The computational results are reported in Table 11. The columns titled

"Deterministic" and "Stochastic" correspond to the improvements of the robust model with respect to the deterministic and stochastic models, respectively. For instances with different scales, the robust model can easily achieve more than 10% improvements in both the average cost and the 95% percentile.

Table 11: Computational results for experiment variants

	Uncapacitated Instances					Capacitated Instances				
$\|N\|$	Deterministic (%)		Stochastic (%)		CPU	Deterministic (%)		Stochastic (%)		CPU
	Avg.	95%	Avg.	95%	(s)	Avg.	95%	Avg.	95%	(s)
40	18.93	20.81	13.88	15.63	77	18.42	20.19	13.59	15.70	802
60	14.25	15.11	13.21	14.08	265	17.20	17.78	12.95	13.56	2324
80	16.91	17.50	14.48	14.79	1598	15.30	15.63	12.14	12.68	7361
100	13.15	14.22	12.52	13.37	3793	16.04	19.65	12.30	16.16	9918

Table 11 also displays the average computational time to solve the robust model with different values of $|N|$ (cf. columns titled "CPU (s)"). Generally speaking, the models can be solved with moderate computational effort. One may notice that it can take more than 3 hours to solve the capacitated model with 100 nodes. Recall that the robust model is proposed to make strategic decisions of location and inventory pre-positioning. Consequently, a few hours' computational time will not compromise the practical value of the robust model. Also note that this experiment solves the robust model by Benders decomposition and the resulting master problems, which are MIP problems, by the IBM ILOG CPLEX solver. We believe that these MIP problems can be solved much more efficiently by a tailor-made algorithm. However, it is beyond the scope of this paper as our focus on developing the solution approach is to deal with the min-max objective function of the robust model instead of the integral constraints.

6 Conclusions

A good location and emergency inventory pre-positioning strategy is critical for disaster relief operations. This paper proposes a min-max robust model that optimizes the location and inventory

stocking decisions in the pre-disaster operations, while taking into account the delivery decisions in the post-disaster operations. The proposed model protects against any disturbance of the uncertain parameters, including demands, usable proportions of pre-positioned inventories, and road link capacities, within pre-specified uncertainty sets. For the sake of practicality, the uncertainty sets are defined based on the most likely values, the upper bounds, and the lower bounds of these random inputs. Parameters named uncertainty budgets are introduced to adjust the uncertainty sets and hence control the level of conservatism of the corresponding robust model.

As the robust model contains uncertainties in both left and right hand sides of its constraints, computationally tractable approaches are developed to obtain its optimal solution. We also derive a closed-form optimal solution for certain special cases that minimize the deprivation cost. The closed-form solution reveals that, among all possible values for the uncertainty budget, setting it to 1 is most likely to pre-position the supplies in more than one location, which potentially reduces the risk through diversification. We illustrate the application of the robust model and evaluate its performance using a case study of the 2010 Yushu earthquake. The case study demonstrates that the robust model, especially with uncertainty budget equal to 1, outperforms the deterministic and stochastic models for the same problem. This observation is further confirmed in an extensive numerical study on networks with up to 100 nodes.

This paper restricts the uncertainty budgets to integers for notational simplicity. Nevertheless, our results can be easily generalized to allow fractional uncertainty budgets. Furthermore, the solution approach proposed in Section 3 focuses on resolving the min-max objective function. The resulting reformulation and the master problem obtained from Benders decomposition remain MIP problems and can be computationally challenging for networks with hundreds of nodes. It is promising to develop efficient tailor-made algorithms for these MIP problems based on their structural properties, which we leave for future research. In addition, when modeling the deprivation cost in Section 3.4, we classify the suffering population into two groups. One group receives emergency supplies from the pre-positioned inventories, whereas the other group has to wait for deliveries from the unaffected areas. All individuals in the same group are assumed to have the same deprivation time and cost, which may fail to capture the difference in deprivation times due to multiple deliveries arriving at different times. We would like to address this issue in a future extension, which also aims to reveal managerial insights of transportation activities in the disaster

relief operations.

Acknowledgment. We would like to thank the Department Editor, the Senior Editor, and the referees for constructive comments that led to this improved version. This research is supported by National Natural Science Foundation of China (No. 71171047, No. 71222103, No. 71525001).

Appendix A. Proofs

This section provides the proofs of all the theorems and propositions in this paper.

A.1 Proof of Proposition 1

Proof: We first show that D is a polytope. For any $i \in N$, the definition of η_i in (8) yields that $\eta_i = (d_i^M - \tilde{d}_i)/(d_i^M - d_i^L) \geq 0 \geq (\tilde{d}_i - d_i^M)/(d_i^U - d_i^M)$ if $\tilde{d}_i \leq d_i^M$ and $\eta_i = (\tilde{d}_i - d_i^M)/(d_i^U - d_i^M) > 0 > (d_i^M - \tilde{d}_i)/(d_i^M - d_i^L)$ if $\tilde{d}_i > d_i^M$. Hence, the set D can be written as

$$\begin{aligned} D &= \left\{ \tilde{\mathbf{d}} \in \mathbb{R}^{|N|} \;\middle|\; \begin{array}{l} \eta_i = \max\left\{ \dfrac{d_i^M - \tilde{d}_i}{d_i^M - d_i^L},\ \dfrac{\tilde{d}_i - d_i^M}{d_i^U - d_i^M} \right\} \ \forall i \in N, \\ \tilde{d}_i \in [d_i^L, d_i^U] \ \forall i \in N,\ \sum_{i \in N} \eta_i \leq \gamma_d \end{array} \right\} \\ &= \left\{ \tilde{\mathbf{d}} \in \mathbb{R}^{|N|} \;\middle|\; \begin{array}{l} \eta_i \geq \dfrac{d_i^M - \tilde{d}_i}{d_i^M - d_i^L} \ \forall i \in N,\ \eta_i \geq \dfrac{\tilde{d}_i - d_i^M}{d_i^U - d_i^M} \ \forall i \in N, \\ \tilde{d}_i \in [d_i^L, d_i^U] \ \forall i \in N,\ \sum_{i \in N} \eta_i \leq \gamma_d \end{array} \right\}. \end{aligned} \tag{20}$$

It is straightforward that the set of vectors $[\tilde{d}_1, \ldots, \tilde{d}_{|N|}, \eta_1, \ldots, \eta_{|N|}]^T \in \mathbb{R}^{2|N|}$ satisfying all the constraints in (20) is a polyhedron. Consequently, D is also a polyhedron. Also note that D is contained in the hyperrectangle $\{\mathbf{d} \in \mathbb{R}^{|N|} \mid d_i^L \leq d_i \leq d_i^U \ \forall i \in N\}$. Thus, D is a polytope.

To complete the proof, it suffices to show that for any vector $\mathbf{c} = [c_1, ..., c_{|N|}]^T \in \mathbb{R}^{|N|}$, there exists some $\mathbf{d} \in V_d$ such that $\mathbf{d} \in \arg\min\{\mathbf{c}^T\mathbf{d} : \mathbf{d} \in D\}$. For any given $\mathbf{c} \in \mathbb{R}^{|N|}$, let

$$Z = \min\left\{\mathbf{c}^T\mathbf{d} : \mathbf{d} \in D\right\} \tag{21}$$

and

$$Z' = \min\left\{ \sum_{i \in N} c_i' \eta_i + \sum_{i \in N} c_i d_i^M : 0 \leq \eta_i \leq 1 \ \forall i \in N,\ \sum_{i \in N} \eta_i \leq \gamma_d \right\}, \tag{22}$$

where

$$c_i' = \begin{cases} -c_i(d_i^M - d_i^L), & \text{if } c_i \geq 0 \\ c_i(d_i^U - d_i^M), & \text{if } c_i < 0 \end{cases} \quad \forall i \in N.$$

Suppose $\boldsymbol{\eta}^* \in \mathbb{R}^{|N|}$ is an optimal solution to (22). Construct a vector $\mathbf{d} \in \mathbb{R}^{|N|}$ such that

$$d_i = \begin{cases} d_i^M - \eta_i^*(d_i^M - d_i^L) \in [d_i^L, d_i^M], & \text{if } c_i \geq 0 \\ d_i^M + \eta_i^*(d_i^U - d_i^M) \in [d_i^M, d_i^U], & \text{if } c_i < 0 \end{cases} \quad \forall i \in N. \tag{23}$$

It is straightforward to show that $\mathbf{d} \in D$, i.e., $\mathbf{d}$ is a feasible solution to (21). Note that

$$\begin{aligned} \mathbf{c}^T\mathbf{d} = \sum_{i\in N} c_i d_i &= \sum_{i\in N:c_i\geq 0} c_i\Big(d_i^M - \eta_i^*(d_i^M - d_i^L)\Big) + \sum_{i\in N:c_i<0} c_i\Big(d_i^M + \eta_i^*(d_i^U - d_i^M)\Big) \\ = -\sum_{i\in N:c_i\geq 0} c_i(d_i^M - d_i^L)\eta_i^* &+ \sum_{i\in N:c_i<0} c_i(d_i^U - d_i^M)\eta_i^* + \sum_{i\in N} c_i d_i^M = \sum_{i\in N} c_i'\eta_i^* + \sum_{i\in N} c_i d_i^M = Z'. \end{aligned} \tag{24}$$

Therefore, we obtain $Z \leq Z'$.

Conversely, suppose $\mathbf{d}^* \in \mathbb{R}^{|N|}$ is an optimal solution to (21). Define a vector $\boldsymbol{\eta} \in \mathbb{R}^{|N|}$ such that

$$\eta_i = \max\left\{\frac{d_i^M - d_i^*}{d_i^M - d_i^L},\ \frac{d_i^* - d_i^M}{d_i^U - d_i^M}\right\} \in [0,1] \quad \forall i \in N,$$

which, by the first equality in (20), is feasible to (22). The objective value of (22) corresponding to $\boldsymbol{\eta}$ is

$$\begin{aligned} \sum_{i\in N} c_i'\eta_i + \sum_{i\in N} c_i d_i^M &= -\sum_{i\in N:c_i\geq 0} c_i(d_i^M - d_i^L)\eta_i + \sum_{i\in N:c_i<0} c_i(d_i^U - d_i^M)\eta_i + \sum_{i\in N} c_i d_i^M \\ \leq -\sum_{i\in N:c_i\geq 0} c_i(d_i^M - d_i^L)\cdot\frac{d_i^M - d_i^*}{d_i^M - d_i^L} &+ \sum_{i\in N:c_i<0} c_i(d_i^U - d_i^M)\cdot\frac{d_i^* - d_i^M}{d_i^U - d_i^M} + \sum_{i\in N} c_i d_i^M \\ = -\sum_{i\in N:c_i\geq 0} c_i(d_i^M - d_i^*) &+ \sum_{i\in N:c_i<0} c_i(d_i^* - d_i^M) + \sum_{i\in N} c_i d_i^M = \sum_{i\in N} c_i d_i^* = \mathbf{c}^T\mathbf{d}^* = Z, \end{aligned}$$

which yields $Z' \leq Z$. Recall that $Z \leq Z'$. It follows that (21) and (22) are equivalent.

By sorting c_i' for all $i \in N$, we can obtain $\{i_1, i_2, ..., i_{|N|}\}$ such that $\{i_1, i_2, ..., i_{|N|}\} = N$ and $c_{i_1}' \leq c_{i_2}' \leq \cdots \leq c_{i_{|N|}}'$. Let $T = \{i_1, i_2, ..., i_{\gamma_d}\}$. Obviously, as $c_i' \leq 0$ for all $i \in N$, an optimal solution $\boldsymbol{\eta}^*$ to (22) is $\eta_i^* = 1$ for all $i \in T$ and $\eta_i^* = 0$ for all $i \in N \setminus T$. Consider the corresponding $\mathbf{d}$ defined by (23). Note that $\mathbf{d}$ is feasible to (21). According to the equivalence between (21) and

(22), (24) implies that $\mathbf{d}$ is an optimal solution to (21). (23) yields that

$$d_i = \begin{cases} d_i^L, \text{ if } c_i \geq 0 \\ d_i^U, \text{ if } c_i < 0 \end{cases} \quad \forall i \in T \qquad \text{and} \qquad d_i = d_i^M \quad \forall i \in N \setminus T.$$

$T \subseteq N$ and $|T| = \gamma_d$ immediately imply $\mathbf{d} \in V_d$, which completes the proof. □

A.2 Proof of Theorem 2

Proof: By adopting the dual variable $\boldsymbol{\alpha}$, the dual of (15) is

$$\max \left\{ \left(\boldsymbol{\Xi} \tilde{\mathbf{b}}_2 + \boldsymbol{\xi} - (\boldsymbol{\Phi} \tilde{\mathbf{A}}_2 + \boldsymbol{\Psi}) \mathbf{x}_1 \right)^T \boldsymbol{\alpha} : \mathbf{B}^T \boldsymbol{\alpha} \leq \mathbf{c}_2 \right\}. \tag{25}$$

Recall that $\mathcal{Q}(\mathbf{x}_1, \tilde{\mathbf{A}}_2, \tilde{\mathbf{b}}_2)$ has an optimal solution for some $\tilde{\mathbf{A}}_2 \in M_A$ and $\tilde{\mathbf{b}}_2 \in M_b$. Thus, the dual problem (25) for this pair of $\tilde{\mathbf{A}}_2$ and $\tilde{\mathbf{b}}_2$ must be feasible. As the constraint $\mathbf{B}^T \boldsymbol{\alpha} \leq \mathbf{c}_2$ is independent of $\tilde{\mathbf{A}}_2$ and $\tilde{\mathbf{b}}_2$, the dual (25) is feasible for all $\tilde{\mathbf{A}}_2 \in M_A$ and $\tilde{\mathbf{b}}_2 \in M_b$. Also note that the primal (15) is feasible for all $\tilde{\mathbf{A}}_2 \in M_A$ and $\tilde{\mathbf{b}}_2 \in M_b$. Consequently, we obtain

$$\mathcal{Q}(\mathbf{x}_1, \tilde{\mathbf{A}}_2, \tilde{\mathbf{b}}_2) = \max \left\{ \left(\boldsymbol{\Xi} \tilde{\mathbf{b}}_2 + \boldsymbol{\xi} - (\boldsymbol{\Phi} \tilde{\mathbf{A}}_2 + \boldsymbol{\Psi}) \mathbf{x}_1 \right)^T \boldsymbol{\alpha} : \mathbf{B}^T \boldsymbol{\alpha} \leq \mathbf{c}_2 \right\}, \tag{26}$$

for all $\tilde{\mathbf{A}}_2 \in M_A$ and $\tilde{\mathbf{b}}_2 \in M_b$, which yields

$$\begin{aligned} & \max_{\tilde{\mathbf{A}}_2 \in M_A, \tilde{\mathbf{b}}_2 \in M_b} \mathcal{Q}(\mathbf{x}_1, \tilde{\mathbf{A}}_2, \tilde{\mathbf{b}}_2) \\ &= \max \left\{ \left(\boldsymbol{\Xi} \tilde{\mathbf{b}}_2 + \boldsymbol{\xi} - (\boldsymbol{\Phi} \tilde{\mathbf{A}}_2 + \boldsymbol{\Psi}) \mathbf{x}_1 \right)^T \boldsymbol{\alpha} : \tilde{\mathbf{A}}_2 \in M_A, \tilde{\mathbf{b}}_2 \in M_b, \mathbf{B}^T \boldsymbol{\alpha} \leq \mathbf{c}_2 \right\} \\ &= \max \left\{ \max_{\tilde{\mathbf{A}}_2 \in M_A, \tilde{\mathbf{b}}_2 \in M_b} \left(\boldsymbol{\Xi} \tilde{\mathbf{b}}_2 + \boldsymbol{\xi} - (\boldsymbol{\Phi} \tilde{\mathbf{A}}_2 + \boldsymbol{\Psi}) \mathbf{x}_1 \right)^T \boldsymbol{\alpha} : \mathbf{B}^T \boldsymbol{\alpha} \leq \mathbf{c}_2 \right\}. \end{aligned}$$

As M_A and M_b are polyhedra, for any given $\boldsymbol{\alpha}$,

$$\max_{\tilde{\mathbf{A}}_2 \in M_A, \tilde{\mathbf{b}}_2 \in M_b} \left(\boldsymbol{\Xi} \tilde{\mathbf{b}}_2 + \boldsymbol{\xi} - (\boldsymbol{\Phi} \tilde{\mathbf{A}}_2 + \boldsymbol{\Psi}) \mathbf{x}_1 \right)^T \boldsymbol{\alpha}$$

is a linear program. Note that $V_A \subseteq M_A$ and $V_b \subseteq M_b$ are supersets of the vertices of M_A and M_b, respectively. The boundedness of M_A and M_b yields

$$\max_{\tilde{\mathbf{A}}_2 \in M_A, \tilde{\mathbf{b}}_2 \in M_b} \left(\boldsymbol{\Xi} \tilde{\mathbf{b}}_2 + \boldsymbol{\xi} - (\boldsymbol{\Phi} \tilde{\mathbf{A}}_2 + \boldsymbol{\Psi}) \mathbf{x}_1 \right)^T \boldsymbol{\alpha} = \max_{\tilde{\mathbf{A}}_2 \in V_A, \tilde{\mathbf{b}}_2 \in V_b} \left(\boldsymbol{\Xi} \tilde{\mathbf{b}}_2 + \boldsymbol{\xi} - (\boldsymbol{\Phi} \tilde{\mathbf{A}}_2 + \boldsymbol{\Psi}) \mathbf{x}_1 \right)^T \boldsymbol{\alpha}.$$

As a result,

$$\begin{aligned}
&\max_{\tilde{\mathbf{A}}_2\in M_A,\tilde{\mathbf{b}}_2\in M_b} \mathcal{Q}(\mathbf{x}_1,\tilde{\mathbf{A}}_2,\tilde{\mathbf{b}}_2)\\
&= \max\left\{\max_{\tilde{\mathbf{A}}_2\in V_A,\tilde{\mathbf{b}}_2\in V_b}\left(\boldsymbol{\Xi}\tilde{\mathbf{b}}_2+\boldsymbol{\xi}-(\boldsymbol{\Phi}\tilde{\mathbf{A}}_2+\boldsymbol{\Psi})\mathbf{x}_1\right)^T\boldsymbol{\alpha}:\mathbf{B}^T\boldsymbol{\alpha}\le\mathbf{c}_2\right\}\\
&= \max\left\{\left(\boldsymbol{\Xi}\tilde{\mathbf{b}}_2+\boldsymbol{\xi}-(\boldsymbol{\Phi}\tilde{\mathbf{A}}_2+\boldsymbol{\Psi})\mathbf{x}_1\right)^T\boldsymbol{\alpha}:\tilde{\mathbf{A}}_2\in V_A,\tilde{\mathbf{b}}_2\in V_b,\mathbf{B}^T\boldsymbol{\alpha}\le\mathbf{c}_2\right\}\\
&= \max_{\tilde{\mathbf{A}}_2\in V_A,\tilde{\mathbf{b}}_2\in V_b} \mathcal{Q}(\mathbf{x}_1,\tilde{\mathbf{A}}_2,\tilde{\mathbf{b}}_2),
\end{aligned}$$

where the last inequality follows from (26). Therefore, (14) and (16) are equivalent. □

A.3 Proof of Proposition 3

Proof: Obviously, Proposition 3 holds as long as

$$\max_{\tilde{\mathbf{d}}\in V_d,\tilde{\boldsymbol{\rho}}\in V_\rho,\tilde{\mathbf{u}}\in V_u}\mathcal{Q}(\mathbf{r},\tilde{\mathbf{d}},\tilde{\boldsymbol{\rho}},\tilde{\mathbf{u}})=\max_{(\tilde{\mathbf{d}},\tilde{\boldsymbol{\rho}})\in V_{(d,\rho)},\tilde{\mathbf{u}}\in\bar{V}_u}\mathcal{Q}(\mathbf{r},\tilde{\mathbf{d}},\tilde{\boldsymbol{\rho}},\tilde{\mathbf{u}}),\quad\forall\mathbf{r}\ge\mathbf{0},$$

i.e., for any $\mathbf{r}\ge\mathbf{0}$, $\mathbf{d}\in V_d$, $\boldsymbol{\rho}\in V_\rho$, and $\mathbf{u}\in V_u$, there exists some $(\mathbf{d}',\boldsymbol{\rho}')\in V_{(d,\rho)}$ and $\mathbf{u}'\in\bar{V}_u$ such that $\mathcal{Q}(\mathbf{r},\mathbf{d},\boldsymbol{\rho},\mathbf{u})\le\mathcal{Q}(\mathbf{r},\mathbf{d}',\boldsymbol{\rho}',\mathbf{u}')$.

Consider any arbitrary $\mathbf{r}\ge\mathbf{0}$, $\mathbf{d}\in V_d$, $\boldsymbol{\rho}\in V_\rho$, and $\mathbf{u}\in V_u$. Applying the derivation of (26), we can show that

$$\mathcal{Q}(\mathbf{r},\tilde{\mathbf{d}},\tilde{\boldsymbol{\rho}},\tilde{\mathbf{u}})=\max\left\{\sum_{i\in N}(\tilde{d}_i-\tilde{\rho}_i r_i)\alpha_i+\sum_{(i,j)\in A}\tilde{u}_{ij}\beta_{ij}:(\boldsymbol{\alpha},\boldsymbol{\beta})\in F\right\},\quad\forall\tilde{\mathbf{d}}\in V_d,\tilde{\boldsymbol{\rho}}\in V_\rho,\tilde{\mathbf{u}}\in V_u,\tag{27}$$

where

$$F=\left\{(\boldsymbol{\alpha},\boldsymbol{\beta})\;\middle|\;\begin{array}{l}-q_i^+\le\alpha_i\le q_i^-\;\forall i\in N,\;\beta_{ij}+\alpha_j-\alpha_i\le c_{ij}\;\forall(i,j)\in A,\\ \beta_{ij}\le 0\;\forall(i,j)\in A,\;\boldsymbol{\alpha}\in\mathbb{R}^{|N|},\;\boldsymbol{\beta}\in\mathbb{R}^{|A|}\end{array}\right\}.\tag{28}$$

Furthermore, (27) has an optimal solution for any $\tilde{\mathbf{d}}\in V_d$, $\tilde{\boldsymbol{\rho}}\in V_\rho$, and $\tilde{\mathbf{u}}\in V_u$. Therefore, for the given $\mathbf{r}$, $\mathbf{d}$, $\boldsymbol{\rho}$, and $\mathbf{u}$, there exists $(\boldsymbol{\alpha}^*,\boldsymbol{\beta}^*)\in F$ such that

$$\mathcal{Q}(\mathbf{r},\mathbf{d},\boldsymbol{\rho},\mathbf{u})=\sum_{i\in N}(d_i-\rho_i r_i)\alpha_i^*+\sum_{(i,j)\in A}u_{ij}\beta_{ij}^*.$$

Let $N_+=\left\{i\in N:d_i>d_i^M,\;\rho_i>\rho_i^M\right\}$ and $N_-=\left\{i\in N:d_i<d_i^M,\;\rho_i<\rho_i^M\right\}$. We can define

$\mathbf{d}'$ and $\boldsymbol{\rho}'$ such that

$$(d_i', \rho_i') = \begin{cases} (d_i, \rho_i^L), & \forall i \in N_+ \text{ and } \alpha_i^* \geq 0, \\ (d_i^L, \rho_i), & \forall i \in N_+ \text{ and } \alpha_i^* < 0, \\ (d_i^U, \rho_i), & \forall i \in N_- \text{ and } \alpha_i^* \geq 0, \\ (d_i, \rho_i^U), & \forall i \in N_- \text{ and } \alpha_i^* < 0, \\ (d_i, \rho_i), & \forall i \in N \setminus N_+ \setminus N_-. \end{cases}$$

As $r_i \geq 0$, it is straightforward that $(d_i - \rho_i r_i)\alpha_i^* \leq (d_i' - \rho_i' r_i)\alpha_i^*$ for all $i \in N$. Moreover, let $A_+ = \{(i,j) \in A : u_{ij} > u_{ij}^M\}$ and

$$u_{ij}' = \begin{cases} u_{ij}^L \leq u_{ij}^M < u_{ij}, & \forall (i,j) \in A_+, \\ u_{ij}, & \forall (i,j) \in A \setminus A_+, \end{cases}$$

which, as $\beta_{ij}^* \leq 0$, immediately yields $u_{ij}\beta_{ij}^* \leq u_{ij}'\beta_{ij}^*$ for all $(i,j) \in A$. Therefore, we obtain

$$\mathcal{Q}(\mathbf{r}, \mathbf{d}, \boldsymbol{\rho}, \mathbf{u}) = \sum_{i \in N}(d_i - \rho_i r_i)\alpha_i^* + \sum_{(i,j) \in A} u_{ij}\beta_{ij}^* \leq \sum_{i \in N}(d_i' - \rho_i' r_i)\alpha_i^* + \sum_{(i,j) \in A} u_{ij}'\beta_{ij}^* \leq \mathcal{Q}(\mathbf{r}, \mathbf{d}', \boldsymbol{\rho}', \mathbf{u}'),$$

where the last inequality follows from that $(\boldsymbol{\alpha}^*, \boldsymbol{\beta}^*) \in F$ is a feasible solution to the optimization problem $\mathcal{Q}(\mathbf{r}, \mathbf{d}', \boldsymbol{\rho}', \mathbf{u}')$ in (27). Applying the definitions of V_d, V_ρ, V_u, $V_{(d,\rho)}$, and $\bar{V}_u$, the definitions of $\mathbf{d}'$, $\boldsymbol{\rho}'$, and $\mathbf{u}'$ imply that $(\mathbf{d}', \boldsymbol{\rho}') \in V_{(d,\rho)}$ and $\mathbf{u}' \in \bar{V}_u$, which completes the proof. □

A.4 Proof of Proposition 4

Proof: Consider any given $\mathbf{r} \geq \mathbf{0}$. Note that

$$\max_{(\tilde{\mathbf{d}}, \tilde{\boldsymbol{\rho}}) \in V_{(d,\rho)}, \tilde{\mathbf{u}} \in \bar{V}_u} \mathcal{Q}(\mathbf{r}, \tilde{\mathbf{d}}, \tilde{\boldsymbol{\rho}}, \tilde{\mathbf{u}}) = \max_{\tilde{\mathbf{d}} \in D, \tilde{\boldsymbol{\rho}} \in P, \tilde{\mathbf{u}} \in U} \mathcal{Q}(\mathbf{r}, \tilde{\mathbf{d}}, \tilde{\boldsymbol{\rho}}, \tilde{\mathbf{u}}) \geq \max_{(\tilde{\mathbf{d}}, \tilde{\boldsymbol{\rho}}) \in \bar{V}_{(d,\rho)}(\mathbf{r}), \tilde{\mathbf{u}} \in \bar{V}_u} \mathcal{Q}(\mathbf{r}, \tilde{\mathbf{d}}, \tilde{\boldsymbol{\rho}}, \tilde{\mathbf{u}}),$$

where the equality follows from the proofs of Theorem 2 and Proposition 3 and the inequality is obtained from $\bar{V}_{(d,\rho)}(\mathbf{r}) \times \bar{V}_u \subseteq D \times P \times U$. Therefore, it is sufficient to prove that

$$\max_{(\tilde{\mathbf{d}}, \tilde{\boldsymbol{\rho}}) \in V_{(d,\rho)}, \tilde{\mathbf{u}} \in \bar{V}_u} \mathcal{Q}(\mathbf{r}, \tilde{\mathbf{d}}, \tilde{\boldsymbol{\rho}}, \tilde{\mathbf{u}}) \leq \max_{(\tilde{\mathbf{d}}, \tilde{\boldsymbol{\rho}}) \in \bar{V}_{(d,\rho)}(\mathbf{r}), \tilde{\mathbf{u}} \in \bar{V}_u} \mathcal{Q}(\mathbf{r}, \tilde{\mathbf{d}}, \tilde{\boldsymbol{\rho}}, \tilde{\mathbf{u}}),$$

i.e., for any $(\mathbf{d}, \boldsymbol{\rho}) \in V_{(d,\rho)}$ and $\mathbf{u} \in \bar{V}_u$, there exists some $(\mathbf{d}', \boldsymbol{\rho}') \in \bar{V}_{(d,\rho)}(\mathbf{r})$ such that $\mathcal{Q}(\mathbf{r}, \mathbf{d}, \boldsymbol{\rho}, \mathbf{u}) \leq \mathcal{Q}(\mathbf{r}, \mathbf{d}', \boldsymbol{\rho}', \mathbf{u})$.

For any given $\mathbf{d}$, $\boldsymbol{\rho}$, and $\mathbf{u}$, as shown in the proof of Proposition 3, there exists $(\boldsymbol{\alpha}^*, \boldsymbol{\beta}^*) \in F$ such that

$$\mathcal{Q}(\mathbf{r}, \mathbf{d}, \boldsymbol{\rho}, \mathbf{u}) = \sum_{i \in N} (d_i - \rho_i r_i)\alpha_i^* + \sum_{(i,j) \in A} u_{ij}\beta_{ij}^*,$$

where F is defined in (28). Let $N_+ = \{i \in N : r_i > 0\}$ and $N'_+ = \{i \in N : r_i > 0, \rho_i \neq \rho_i^M\}$. Note that $|N'_+| \leq \bar{\gamma}_\rho(\mathbf{r}) \leq |N_+|$. Therefore, we can choose $S \subseteq N_+ \setminus N'_+$ such that $|S| = \bar{\gamma}_\rho(\mathbf{r}) - |N'_+|$. Define $\mathbf{d}'$ and $\boldsymbol{\rho}'$ such that

$$(d'_i, \rho'_i) = \begin{cases} (d_i, \rho_i), & \forall i \in N_+ \setminus S, \\ (d_i, \rho_i^L), & \forall i \in S,\ d_i = d_i^M,\ \text{and } \alpha_i^* \geq 0, \\ (d_i, \rho_i^U), & \forall i \in S,\ d_i = d_i^M,\ \text{and } \alpha_i^* < 0, \\ (d_i^U, \rho_i^L), & \forall i \in S,\ d_i \neq d_i^M,\ \text{and } \alpha_i^* \geq 0, \\ (d_i^L, \rho_i^U), & \forall i \in S,\ d_i \neq d_i^M,\ \text{and } \alpha_i^* < 0, \\ (d_i, \rho_i^M) & \forall i \in N \setminus N_+. \end{cases}$$

It is straightforward to verify that $(\mathbf{d}', \boldsymbol{\rho}') \in \bar{V}_{(d,\rho)}(\mathbf{r})$ and $(d_i - \rho_i r_i)\alpha_i^* \leq (d'_i - \rho'_i r_i)\alpha_i^*$ for all $i \in N$. As in the proof of Proposition 3, we obtain

$$\mathcal{Q}(\mathbf{r}, \mathbf{d}, \boldsymbol{\rho}, \mathbf{u}) = \sum_{i \in N} (d_i - \rho_i r_i)\alpha_i^* + \sum_{(i,j) \in A} u_{ij}\beta_{ij}^* \leq \sum_{i \in N} (d'_i - \rho'_i r_i)\alpha_i^* + \sum_{(i,j) \in A} u_{ij}\beta_{ij}^* \leq \mathcal{Q}(\mathbf{r}, \mathbf{d}', \boldsymbol{\rho}', \mathbf{u})$$

since $(\boldsymbol{\alpha}^*, \boldsymbol{\beta}^*) \in F$ is feasible to the optimization problem $\mathcal{Q}(\mathbf{r}, \mathbf{d}', \boldsymbol{\rho}', \mathbf{u})$ in (27). □

A.5 Proof of Theorem 5

Proof: As $\mathcal{G}(N, A)$ is uncapacitated, we can drop $\tilde{\mathbf{u}}$ in $\mathcal{Q}(\mathbf{r}, \tilde{\mathbf{d}}, \tilde{\boldsymbol{\rho}}, \tilde{\mathbf{u}})$ defined in (4). Furthermore, applying $q_i^+ = 0$ for all $i \in N$ and $c_{ij} = 0$ for all $(i, j) \in A$, the dual problem of $\mathcal{Q}(\mathbf{r}, \tilde{\mathbf{d}}, \tilde{\boldsymbol{\rho}})$ in (27) can be reduced to

$$\mathcal{Q}(\mathbf{r}, \tilde{\mathbf{d}}, \tilde{\boldsymbol{\rho}}) = \max \left\{ \sum_{i \in N} (\tilde{d}_i - \tilde{\rho}_i r_i)\alpha_i : \alpha_j - \alpha_i \leq 0\ \forall (i,j) \in A,\ 0 \leq \alpha_i \leq q_i^-\ \forall i \in N \right\}.$$

For any $i, j \in N$, if there exists a directed path in $\mathcal{G}(N, A)$ from i to j, the first constraint in the dual of $\mathcal{Q}(\mathbf{r}, \mathbf{d}, \boldsymbol{\rho})$ implies that $\alpha_j \leq \alpha_i$. Recall that $\mathcal{G}(N, A)$ is strongly connected, i.e., there

exists a directed path between any two nodes in N. Therefore, any feasible solution to the dual of $\mathcal{Q}(\mathbf{r}, \mathbf{d}, \boldsymbol{\rho})$ should satisfy $\alpha_i = \alpha_j$ for any $i, j \in N$, i.e.,

$$\mathcal{Q}(\mathbf{r}, \tilde{\mathbf{d}}, \tilde{\boldsymbol{\rho}}) = \max\left\{\sum_{i\in N}(\tilde{d}_i - \tilde{\rho}_i r_i)\alpha : 0 \le \alpha \le q_i^- \ \forall i \in N\right\} = \max\left\{0, q^-\left(\sum_{i\in N}(\tilde{d}_i - \tilde{\rho}_i r_i)\right)\right\},$$

where $q^- = \min\{q_i^- : i \in N\} \ge 0$.

Applying the conditions that $\mathcal{G}(N, A)$ is uncapacitated and $F_i = h_i = q_i^+ = 0$ for all $i \in N$, it is straightforward that model (7) can be simplified to

$$\min_{\substack{\sum_{i\in N} r_i = R,\\ r_i \ge 0 \ \forall i\in N}}\left\{\max_{\tilde{\mathbf{d}}\in D, \tilde{\boldsymbol{\rho}}\in P}\left\{\max\left\{0, q^-\left(\sum_{i\in N}(\tilde{d}_i - \tilde{\rho}_i r_i)\right)\right\}\right\}\right\}$$

with $y_i = 1$ for all $i \in N$. Also note that the objective function is increasing in $\sum_{i\in N}(\tilde{d}_i - \tilde{\rho}_i r_i)$. An optimal solution to model (7) can be obtained by solving

$$\begin{aligned}\min_{\substack{\sum_{i\in N} r_i = R,\\ r_i \ge 0 \ \forall i\in N}}\left\{\max_{\tilde{\mathbf{d}}\in D, \tilde{\boldsymbol{\rho}}\in P}\left\{\sum_{i\in N}(\tilde{d}_i - \tilde{\rho}_i r_i)\right\}\right\} &= \min_{\substack{\sum_{i\in N} r_i = R,\\ r_i \ge 0 \ \forall i\in N}}\left\{\max_{\tilde{\mathbf{d}}\in D}\left\{\sum_{i\in N}\tilde{d}_i\right\} - \min_{\tilde{\boldsymbol{\rho}}\in P}\left\{\sum_{i\in N}\tilde{\rho}_i r_i\right\}\right\}\\ &= \max_{\tilde{\mathbf{d}}\in D}\left\{\sum_{i\in N}\tilde{d}_i\right\} - \max_{\substack{\sum_{i\in N} r_i = R,\\ r_i \ge 0 \ \forall i\in N}}\left\{\min_{\tilde{\boldsymbol{\rho}}\in P}\left\{\sum_{i\in N}\tilde{\rho}_i r_i\right\}\right\},\end{aligned}$$

i.e., it is sufficient to consider

$$\max_{\substack{\sum_{i\in N} r_i = R,\\ r_i \ge 0 \ \forall i\in N}}\left\{\min_{\tilde{\boldsymbol{\rho}}\in P}\left\{\sum_{i\in N}\tilde{\rho}_i r_i\right\}\right\}. \tag{29}$$

Note that

$$\min_{\tilde{\boldsymbol{\rho}}\in P}\left\{\sum_{i\in N}\tilde{\rho}_i r_i\right\} = \begin{cases}\sum_{i\in N}\rho_i^M r_i, & \text{if } \gamma_\rho = 0,\\ \min_{\rho_i^L \le \tilde{\rho}_i \le \rho_i^U \forall i\in N}\left\{\sum_{i\in N}\tilde{\rho}_i r_i\right\} = \sum_{i\in N}\rho_i^L r_i, & \text{if } \gamma_\rho = |N|,\end{cases}$$

which immediately implies the results for $\gamma_\rho \in \{0, |N|\}$.

Consider $\gamma_\rho \in \{1, ..., |N| - 1\}$. As shown in the proof of Proposition 1, $r_i \ge 0$ for all $i \in N$ implies

$$\min_{\tilde{\boldsymbol{\rho}}\in P}\left\{\sum_{i\in N}\tilde{\rho}_i r_i\right\} = \min\left\{\sum_{i\in N}\rho_i^M r_i - \sum_{i\in N}(\rho_i^M - \rho_i^L) r_i \eta_i : 0 \le \eta_i \le 1 \ \forall i \in N, \ \sum_{i\in N}\eta_i \le \gamma_\rho\right\}.$$

Suppose that $\sigma : \{1, ..., |N|\} \mapsto N$ is a permutation of N. Given

$$(\rho_{\sigma(1)}^M - \rho_{\sigma(1)}^L) r_{\sigma(1)} \ge (\rho_{\sigma(2)}^M - \rho_{\sigma(2)}^L) r_{\sigma(2)} \ge \cdots \ge (\rho_{\sigma(|N|)}^M - \rho_{\sigma(|N|)}^L) r_{\sigma(|N|)},$$

we obtain

$$\min_{\tilde{\boldsymbol{\rho}}\in P}\left\{\sum_{i\in N}\tilde{\rho}_i r_i\right\} = \sum_{i\in N}\rho_i^M r_i - \sum_{i=1}^{\gamma_\rho}(\rho_{\sigma(i)}^M - \rho_{\sigma(i)}^L)r_{\sigma(i)} = \sum_{i=1}^{\gamma_\rho}\rho_{\sigma(i)}^L r_{\sigma(i)} + \sum_{i=\gamma_\rho+1}^{|N|}\rho_{\sigma(i)}^M r_{\sigma(i)}.$$

Let Σ denote the set of permutations of N. Model (29) is equivalent to $\max\{z(\sigma) : \sigma \in \Sigma\}$, where

$$\begin{aligned} z(\sigma) = \max \quad & \textstyle\sum_{i=1}^{\gamma_\rho}\rho_{\sigma(i)}^L r_{\sigma(i)} + \sum_{i=\gamma_\rho+1}^{|N|}\rho_{\sigma(i)}^M r_{\sigma(i)} \\ \text{s.t.} \quad & \textstyle\sum_{i=1}^{|N|} r_{\sigma(i)} = R, \\ & (\rho_{\sigma(1)}^M - \rho_{\sigma(1)}^L)r_{\sigma(1)} \geq (\rho_{\sigma(2)}^M - \rho_{\sigma(2)}^L)r_{\sigma(2)} \geq \cdots \geq (\rho_{\sigma(|N|)}^M - \rho_{\sigma(|N|)}^L)r_{\sigma(|N|)} \geq 0. \end{aligned}$$

Applying strong duality, we obtain

$$\begin{aligned} z(\sigma) = \min \quad & R\beta \\ \text{s.t.} \quad & \beta - (\rho_{\sigma(1)}^M - \rho_{\sigma(1)}^L)\alpha_1 = \rho_{\sigma(1)}^L, \\ & \beta - (\rho_{\sigma(i)}^M - \rho_{\sigma(i)}^L)\alpha_i + (\rho_{\sigma(i)}^M - \rho_{\sigma(i)}^L)\alpha_{i-1} = \rho_{\sigma(i)}^L, \quad \forall i \in \{2, ..., \gamma_\rho\}, \\ & \beta - (\rho_{\sigma(i)}^M - \rho_{\sigma(i)}^L)\alpha_i + (\rho_{\sigma(i)}^M - \rho_{\sigma(i)}^L)\alpha_{i-1} = \rho_{\sigma(i)}^M, \quad \forall i \in \{\gamma_\rho + 1, ..., N\}, \\ & \alpha_i \geq 0, \quad \forall i \in \{1, ..., |N|\}. \end{aligned}$$

Note that the equality constraints in the above problem are equivalent to

$$\begin{aligned} &\sum_{j=1}^{i}\frac{1}{\rho_{\sigma(j)}^M - \rho_{\sigma(j)}^L}\beta - \alpha_i = \sum_{j=1}^{i}\frac{\rho_{\sigma(j)}^L}{\rho_{\sigma(j)}^M - \rho_{\sigma(j)}^L}, \quad \forall i \in \{1, ..., \gamma_\rho\}, \\ &\sum_{j=1}^{i}\frac{1}{\rho_{\sigma(j)}^M - \rho_{\sigma(j)}^L}\beta - \alpha_i = \sum_{j=1}^{\gamma_\rho}\frac{\rho_{\sigma(j)}^L}{\rho_{\sigma(j)}^M - \rho_{\sigma(j)}^L} + \sum_{j=\gamma_\rho+1}^{i}\frac{\rho_{\sigma(j)}^M}{\rho_{\sigma(j)}^M - \rho_{\sigma(j)}^L}, \quad \forall i \in \{\gamma_\rho + 1, ..., |N|\}. \end{aligned}$$

To simplify the notation, let $\pi_i = \left(\rho_i^M - \rho_i^L\right)^{-1}$ for all $i \in N$. We have

$$\begin{aligned} z(\sigma) &= \min\left\{R\beta : \beta \geq \frac{\sum_{j=1}^{i}\left(\mathbf{1}_{j\leq\gamma_\rho}\rho_{\sigma(j)}^L + \mathbf{1}_{j>\gamma_\rho}\rho_{\sigma(j)}^M\right)\pi_{\sigma(j)}}{\sum_{j=1}^{i}\pi_{\sigma(j)}} \ \forall i \in \{1, ..., |N|\}\right\} \\ &= \max_{i\in\{1,...,|N|\}}\left\{R \cdot \frac{\sum_{j=1}^{i}\left(\mathbf{1}_{j\leq\gamma_\rho}\rho_{\sigma(j)}^L + \mathbf{1}_{j>\gamma_\rho}\rho_{\sigma(j)}^M\right)\pi_{\sigma(j)}}{\sum_{j=1}^{i}\pi_{\sigma(j)}}\right\}. \end{aligned}$$

It is straightforward that an optimal solution to the primal problem of $z(\sigma)$ is $\mathbf{r}(\sigma)$ such that

$$r_i(\sigma) = R \cdot \frac{\pi_{\sigma(i)}}{\sum_{j=1}^{i}\pi_{\sigma(j)}} \ \forall i \in \{1, ..., i(\sigma)\} \quad \text{and} \quad r_i(\sigma) = 0 \ \forall i \in \{i(\sigma) + 1, ..., |N|\}, \tag{30}$$

where

$$i(\sigma) \in \arg\max_{i\in\{1,...,|N|\}}\left\{\frac{\sum_{j=1}^{i}\left(\mathbf{1}_{j\leq\gamma_\rho}\rho_{\sigma(j)}^L + \mathbf{1}_{j>\gamma_\rho}\rho_{\sigma(j)}^M\right)\pi_{\sigma(j)}}{\sum_{j=1}^{i}\pi_{\sigma(j)}}\right\}.$$

Consider the case in part (c). Then we have $\pi_i = 1/\delta$ for all $i \in N$. For any $\sigma \in \Sigma$ and $i \in \{1, ..., |N|\}$,

$$\frac{\sum_{j=1}^{i}\left(\mathbf{1}_{j\le\gamma_\rho}\rho^L_{\sigma(j)} + \mathbf{1}_{j>\gamma_\rho}\rho^M_{\sigma(j)}\right)\pi_{\sigma(j)}}{\sum_{j=1}^{i}\pi_{\sigma(j)}} = \frac{\sum_{j=1}^{i}\left(\rho^M_{\sigma(j)} - \mathbf{1}_{j\le\gamma_\rho}\delta\right)\delta^{-1}}{\sum_{j=1}^{i}\delta^{-1}} = \frac{1}{i}\left(\sum_{j=1}^{i}\rho^M_{\sigma(j)} - \min\{i,\gamma_\rho\}\delta\right).$$

Thus, model (29) can be written as

$$\begin{aligned}\max_{\sigma\in\Sigma}\{z(\sigma)\} &= \max_{\sigma\in\Sigma}\max_{i\in\{1,...,|N|\}}\left\{\frac{R}{i}\left(\sum_{j=1}^{i}\rho^M_{\sigma(j)} - \min\{i,\gamma_\rho\}\delta\right)\right\}\\ &= \max_{i\in\{1,...,|N|\}}\max_{\sigma\in\Sigma}\left\{\frac{R}{i}\left(\sum_{j=1}^{i}\rho^M_{\sigma(j)} - \min\{i,\gamma_\rho\}\delta\right)\right\}.\end{aligned}$$

Applying $\rho^M_1 \ge \rho^M_2 \ge \cdots \ge \rho^M_{|N|}$, we have

$$\max_{\sigma\in\Sigma}\{z(\sigma)\} = \max_{i\in\{1,...,|N|\}}\left\{\frac{R}{i}\left(\sum_{j=1}^{i}\rho^M_{j} - \min\{i,\gamma_\rho\}\delta\right)\right\}.$$

Consequently, part (c) is an immediate result of (30).

Consider the case in part (d), where $\pi_1 \ge \pi_2 \ge \cdots \ge \pi_{|N|}$. For any $\sigma \in \Sigma$ and $i \in \{1, ..., |N|\}$,

$$\frac{\sum_{j=1}^{i}\left(\mathbf{1}_{j\le\gamma_\rho}\rho^L_{\sigma(j)} + \mathbf{1}_{j>\gamma_\rho}\rho^M_{\sigma(j)}\right)\pi_{\sigma(j)}}{\sum_{j=1}^{i}\pi_{\sigma(j)}} = \frac{\sum_{j=1}^{i}\left(\rho^M - \mathbf{1}_{j\le\gamma_\rho}(\rho^M - \rho^L_{\sigma(j)})\right)\pi_{\sigma(j)}}{\sum_{j=1}^{i}\pi_{\sigma(j)}} = \rho^M - \frac{\min\{i,\gamma_\rho\}}{\sum_{j=1}^{i}\pi_{\sigma(j)}}.$$

Similar to the proof of part (c), model (29) can be written as

$$\max_{\sigma\in\Sigma}\{z(\sigma)\} = \max_{i\in\{1,...,|N|\}}\max_{\sigma\in\Sigma}\left\{R\rho^M - R\cdot\frac{\min\{i,\gamma_\rho\}}{\sum_{j=1}^{i}\pi_{\sigma(j)}}\right\} = \max_{i\in\{1,...,|N|\}}\left\{R\rho^M - R\cdot\frac{\min\{i,\gamma_\rho\}}{\sum_{j=1}^{i}\pi_{j}}\right\}.$$

Also note that

$$\arg\max_{i\in\{1,...,|N|\}}\left\{\rho^M - \frac{\min\{i,\gamma_\rho\}}{\sum_{j=1}^{i}\pi_j}\right\} = \arg\min_{i\in\{1,...,|N|\}}\left\{\frac{\min\{i,\gamma_\rho\}}{\sum_{j=1}^{i}\pi_j}\right\}.$$

The result in part (d) also follows from (30).

Consider the case in part (e). Then we have $\pi_1 \le \pi_2 \le \cdots \le \pi_{|N|}$. Furthermore, for any $\sigma \in \Sigma$ and $i \in \{1, ..., |N|\}$,

$$\frac{\sum_{j=1}^{i}\left(\mathbf{1}_{j\le\gamma_\rho}\rho^L_{\sigma(j)} + \mathbf{1}_{j>\gamma_\rho}\rho^M_{\sigma(j)}\right)\pi_{\sigma(j)}}{\sum_{j=1}^{i}\pi_{\sigma(j)}} = \frac{\sum_{j=1}^{i}\left(\rho^L + \mathbf{1}_{j>\gamma_\rho}(\rho^M_{\sigma(j)} - \rho^L)\right)\pi_{\sigma(j)}}{\sum_{j=1}^{i}\pi_{\sigma(j)}} = \rho^L + \frac{(i-\gamma_\rho)^+}{\sum_{j=1}^{i}\pi_{\sigma(j)}}.$$

As in the proofs of parts (c) and (d), model (29) can be written as

$$\max_{\sigma\in\Sigma}\{z(\sigma)\} = \max_{i\in\{1,...,|N|\}} \max_{\sigma\in\Sigma} \left\{ R\rho^L + R\cdot \frac{(i-\gamma_\rho)^+}{\sum_{j=1}^{i}\pi_{\sigma(j)}} \right\} = \max_{i\in\{1,...,|N|\}} \left\{ R\rho^L + R\cdot \frac{(i-\gamma_\rho)^+}{\sum_{j=1}^{i}\pi_{j}} \right\}.$$

The result in part (e) follows from (30) and

$$\arg\max_{i\in\{1,...,|N|\}} \left\{ \rho^L + \frac{(i-\gamma_\rho)^+}{\sum_{j=1}^{i}\pi_j} \right\} = \arg\max_{i\in\{1,...,|N|\}} \left\{ \frac{(i-\gamma_\rho)^+}{\sum_{j=1}^{i}\pi_j} \right\},$$

which completes the proof. □

A.6 Proof of Proposition 6

Proof: Consider $n^*_{\gamma_\rho}$ defined in Theorem 5 (c). For simplicity, let $a_i = \frac{1}{i\delta}\sum_{j=1}^{i}\rho_j^M$ for $i \in \{1,...,|N|\}$. We have

$$n^*_{\gamma_\rho} \in \arg\max_{i\in\{1,...,|N|\}} \left\{ a_i - i^{-1}\min\{i,\gamma_\rho\} \right\}.$$

Consider any $\gamma_\rho, \gamma'_\rho \in \{1,...,|N|-1\}$ such that $\gamma_\rho \le \gamma'_\rho$. If $n^*_{\gamma_\rho} = 1$ is uniquely optimal, then

$$a_1 - 1^{-1}\min\{1,\gamma'_\rho\} = a_1 - 1^{-1}\min\{1,\gamma_\rho\} > a_i - i^{-1}\min\{i,\gamma_\rho\} \ge a_i - i^{-1}\min\{i,\gamma'_\rho\}$$

for all $i \in \{2,...,|N|\}$, where the first inequality is yielded by the unique optimality of $n^*_{\gamma_\rho} = 1$ and the second inequality follows from the property that $i^{-1}\min\{i,\gamma\}$ is nondecreasing in γ for any $i > 0$. Therefore, $n^*_{\gamma'_\rho} = 1$ is also uniquely optimal.

Similarly, consider $n^*_{\gamma_\rho}$ defined in Theorem 5 (d) for some $\gamma_\rho \in \{1,...|N|\}$. For any $\gamma_\rho, \gamma'_\rho \in \{1,...,|N|-1\}$ such that $\gamma_\rho \le \gamma'_\rho$, if $n^*_{\gamma_\rho} = 1$ is uniquely optimal, then

$$\frac{\min\{1,\gamma'_\rho\}}{\sum_{j=1}^{1}(\rho^M-\rho_j^L)^{-1}} = \frac{\min\{1,\gamma_\rho\}}{\sum_{j=1}^{1}(\rho^M-\rho_j^L)^{-1}} < \frac{\min\{i,\gamma_\rho\}}{\sum_{j=1}^{i}(\rho^M-\rho_j^L)^{-1}} \le \frac{\min\{i,\gamma'_\rho\}}{\sum_{j=1}^{i}(\rho^M-\rho_j^L)^{-1}}$$

for all $i \in \{2,...,|N|\}$, i.e., $n^*_{\gamma'_\rho} = 1$ is also uniquely optimal.

Consider $n^*_{\gamma_\rho}$ defined in Theorem 5 (e). As

$$\frac{(i-\gamma_\rho)^+}{\sum_{j=1}^{i}(\rho_j^M-\rho^L)^{-1}} = 0 \ \forall i \in \{1,...,\gamma_\rho\} \text{ and } \frac{(i-\gamma_\rho)^+}{\sum_{j=1}^{i}(\rho_j^M-\rho^L)^{-1}} > 0 \ \forall i \in \{\gamma_\rho+1,...,|N|\},$$

it is straightforward that $n^*_{\gamma_\rho} \ge \gamma_\rho + 1 > 1$. □

Appendix B. Inputs for the Case Study of Yushu Earthquake

This section shows how the inputs are obtained for the case study of the 2010 Yushu earthquake. We first determine some important parameters for a humanitarian relief commodity package and then estimate the costs, proportions of usable inventories, and capacities used in the case study.

B.1 Humanitarian Relief Commodity Package

The emergency supplies delivered to Yushu within 10 days after the earthquake are listed in Table 12. All items and their amounts, except for drinking water, are obtained from Liu et al (2011). The amount of drinking water is estimated based on that of grain and its unit weight includes the weight of packing materials. As the grain sent to Yushu consisted of 20% of rice and 80% of wheat,[4] the price of grain is calculated based on the prices of rice and wheat published by the China National Grain Trade Center. The shelf lives of tent, coat, quilt, coal-heating furnace, and folding bed are estimated by experience. All other information is obtained from the e-commerce websites JD.com, 1688.com, and Taobao.com.

Table 12: Emergency supplies delivered to Yushu within 10 days after the earthquake

Item	Amount	Unit Weight (kg)	Unit Price (yuan)	Shelf Life (year)
Grain	4,600	1,000	2,481.40	1.5
Drinking Water	4,600	1,072	1,605.56	2
Tent	57,000	3.55	299.00	20
Coat	117,000	1	258.00	20
Quilt	207,000	4.5	116.00	20
Ration Food	10,000	11.52	375.00	3
Coal-Heating Furnace	11,000	40	480.00	20
Folding Bed	20,000	17.58	255.00	20

All the emergency supplies in Table 12 are considered as 1,300 humanitarian relief commodity packages, each of which corresponds to one unit of the commodities in our case study. Note that the expected total demand used in the case study is also 1,300. Furthermore, we assume that the

[4]Source: http://www.bjnews.com.cn/news/2010/04/19/27249.html

weight-to-volume ratio of the commodities is equal to the average of the sea, land, and air freight weight-to-volume ratios.[5] Based on the aforementioned, we can compute the annual depreciation cost, weight, and volume for each unit of the commodities, which are 12,795 yuan, 8,992kg, and 17.98m^3, respectively.

B.2 Cost Parameters

This section presents how we determine the cost parameters in the case studies, i.e., F_i, h_i, q_i^+, q_i^- for all $i \in N$ and c_{ij} for all $(i,j) \in A$. Note that each unit of cost in the case study is equivalent to 5,000 yuan. All the distances used in this section is obtained from Google Map.

B.2.1 Commodity Handling Cost h_i and Penalty Cost of Unused Commodity q_i^+

Assume that the annual inventory holding cost consists of the annual depreciation and operating costs, where the latter is set to 10% of the annual depreciation cost. It follows that the annual inventory holding cost for each unit of the commodities equals 14,074 yuan, which is approximately 2.8 units of cost. We consider both the commodity handling cost h_i and the penalty cost for unused commodity q_i^+ as being at the same level as the annual inventory holding cost. Therefore, the values of h_i and q_i^+ in Table 4 are drawn uniformly from the interval $[1.8, 3.8]$.

B.2.2 Fixed Cost F_i

To estimate the fixed cost F_i, we first determine the cost to build a facility, which is 12,515,823 yuan, based on the following information and assumptions.

- Note that the capacity of a facility is 800 and the volume for each unit of the commodities, as shown in Section B.1, is 17.98m^3. The average storage height and the storage utilization ratio are supposed to be 2.4m and 90%, respectively.
- Each facility is assumed to have 70% brick-concrete structure and 30% brick-wood structure, whose construction costs are listed in Wang (2010). In addition, the cost of land is 139 yuan/m^2.[6]

[5] Source: http://www.rohlig.com/infocenter/air-freight/weightvolume-ratio.html
[6] Source: http://crei.com.cn/tudi/ggao.aspx?id=20166891725470

Given an estimated asset life of 15 years, the annual depreciation cost of a facility is 834,388 yuan. We assume that the annual fixed cost to operate a facility is of the same order of magnitude as 120% of the annual depreciation cost, i.e., 1,001,266 yuan, which is roughly 200 units of cost. Therefore, the fixed cost F_i for all $i \in N$ are generated uniformly in $[100, 300]$.

B.2.3 Transportation Cost c_{ij} for Road Links

The road links considered in the case study are shown in Figure 2. We estimate the transportation costs c_{ij} for these road links based on the fact that 2,170 tons of supplies were delivered to Yushu by 119 trucks between 7:49am on April 14, 2010, i.e., the occuring time of the earthquake, to 0:00am on April 17, 2010.[7] Three components are considered to determine the total cost incurred by these deliveries: the labor cost, the fuel cost, and the truck rental cost. As each truck had two drivers,[8] the labor cost can be calculated easily by assuming a wage of 200 yuan per 8 hours per driver. Suppose that all the 119 trucks are homogeneous trucks made by a multinational automaker. The fuel cost can also be obtained using the 6.15 yuan/L fuel price[9] and the 16.09 L/hour fuel consumption rate.[10] The truck rental rate per hour is then set to 120% of the sum of the following three components (converted to a hourly basis).

- The depreciation cost is calculated using the selling price of truck, which is 750,000 yuan, the vehicle acquisition tax at purchase announced by the government of Qinghai Province of China, and a 15 years useful life.
- The annual vehicle and vessel tax is determined by the truck self-weight, i.e., 9.72 tons, and the tax rate announced by the government of Qinghai Province of China.
- The insurance is estimated to be 20,000 yuan annually.

Therefore, the total cost to deliver 2,170 tons of supplies is estimated to be 1,213,327 yuan. As shown in Section B.1, the unit weight of commodities in our case study is 8,992kg and so the average

[7] Source: http://www.sdjt.gov.cn:50080/publish/main/14/2011/20110308212837834253190/20110308212837834253190_.html

[8] Source: http://www.csi.ac.cn/manage/html/4028861611c5c2ba0111c5c558b00001/_content/10_04/16/1271379228430.html

[9] Source: http://energy.cngold.org/chaiyou.html

[10] Source: https://bbs.360che.com/forum.php?mod=viewthread&tid=602726&extra=page%3D1&page=4

transportation cost per unit is 5,028 yuan, which is approximately 1 unit of cost. Consequently, the unit transportation cost c_{ij} for any road link (i, j) shown in Figure 2 is proportional to the distance between nodes i and j and the average of c_{ij} for all road links (i, j) is equal to 1.

B.2.4 Transportation Cost c_{ij} for Helicopter Links

Mi-171 helicopters, with capacity 4,000kg and fuel consumption rate 900 kg/hour,[11] were deployed in the rescue operations after Yushu earthquake.[12] Based on the fuel consumption rate and flight cost of Mi-26 helicopter on Wikipedia,[13] the flight cost of Mi-171 helicopter is estimated to be 26,568 yuan/hour, which takes into account that a smaller aircraft might be less cost-efficient. Assume that each helicopter delivery takes one hour, which includes 50 minutes' in-flight time and 10 minutes' waiting time. The cost to deliver one unit of the commodities by helicopter is 49,771 yuan, which is roughly 10 units of cost. Thus, in Section 4.2, the transportation cost for helicopter links is set to 10.

B.2.5 Penalty Cost of Unsatisfied Demand q_i^-

In this case study, we consider the penalty cost for unsatisfied demand as the cost of getting additional supply from the unaffected areas. Note that emergency supplies were sent to Yushu by air from six airports,[14] whose average distance to Yushu is 1,455km. Based on the air freight rate of 4.8 yuan/kg for the 1,780km distance from Beijing to Xining,[15] the air freight transportation cost from the unaffected areas to Yushu is estimated to be 35,282 yuan for each unit of the commodities. Assume that the supplies are then delivered to the demand nodes via either road or helicopter links with equal probability. Using the transportation costs for road and helicopter links in Sections B.2.3 and B.2.4, the average shortage cost for each unit of unsatisfied demand is 62,682 yuan, i.e., approximately 12.5 units of cost. Therefore, we generate q_i^- for each $i \in N$ uniformly in the interval $[8, 17]$.

[11] Source: http://www.xnslfh.gov.cn/swweb/article_display.asp?ArticleID=468
[12] Source: http://www.scio.gov.cn/ztk/xwfb/06/6/Document/606117/606117.htm
[13] Source: https://zh.wikipedia.org/wiki/Mi-26%E7%9B%B4%E5%8D%87%E6%9C%BA
[14] Source: http://news.xinhuanet.com/mil/2010-04/16/content_13364417.htm
[15] Source: http://www.zsx56.com/recruitment2.asp

B.3 Proportion of Usable Inventory after Disaster

B.3.1 Predicted Means $\hat{\mu}_i^\rho$

Wang (2010) considers different levels to measure the damage to buildings caused by Yushu earthquake and suggests the percentages of brick-concrete and brick-wood structures in each level of damage severity shown in Table 13. Similar to Xu et al. (2011), we estimate the proportion of inventory, if stored in a building with a given level of damage, that would remain usable after the earthquake, which is also displayed in Table 13. Recall that Section B.2.2 assumes each facility has 70% brick-concrete structure and 30% brick-wood structure. The average proportion of usable inventory can be estimated to be 0.5. Hence, we generate the predicted mean of the proportion of usable inventory $\hat{\mu}_i^\rho$ for each $i \in N$ following a uniform distribution in the interval $[0.4, 0.6]$.

Table 13: Percentages of structures in different levels of damage severity and proportions of usable inventory corresponding to the levels of damage severity

Level of Damage Severity	Devastating	Severe	Moderate	Mild
Brick-Concrete Structure	8.73%	38.19%	20.14%	0.45%
Brick-Wood Structure	12.05%	17.41%	15.89%	15.16%
Proportion of Usable Inventory	0	0.15	0.4	0.7

B.3.2 Actual Means μ_i^ρ

The 13 nodes considered in the case study can be divided into three categories depending on the seismic intensity (cf. Figure 1). The first category consists of nodes 1 and 2, where the seismic intensity is of scale at least VII. Based on the announcement of the State Council Information Office of China,[16] we can estimate the percentages of brick-concrete and brick-wood structures at nodes 1 and 2 that should have been in each level of damage severity considered in Table 13. The estimates are shown in Table 14. As in Section B.3.1, the average proportion of usable inventory at nodes 1 and 2 should be around 0.05. Recall that the average of $\hat{\mu}_i^\rho$ for all $i \in N$ obtained in Section B.3.1 is approximately 0.5. Thus, we set $\mu_i^\rho = 0.1 \times \hat{\mu}_i^\rho$ for all $i \in \{1, 2\}$.

[16] Source: http://www.scio.gov.cn/34473/34576/34516/Document/1477358/1477358.htm

Table 14: Percentages of structures at Nodes 1 and 2 in different levels of damage severity

Level of Damage Severity	Devastating	Severe	Moderate	Mild
Brick-Concrete Structure	80%	15%	5%	3%
Brick-Wood Structure	80%	20%	0%	0%

The second category corresponds to nodes 3, 4, and 5, whose seismic intensity is between VI and VII. The remaining nodes, i.e., nodes 6 to 13, belong to the third category and the corresponding seismic intensity is below VI. Wang (2010) presents the estimated costs for housing reconstruction at nodes 3 to 8, respectively, implying that housing reconstruction at a second category node costs approximately 3.45 times of that at a third category node. Therefore, it is assumed that the average proportion of usable inventory at the third category nodes is 3.45 times of that at the second category nodes. As the average of $\hat{\mu}_i^\rho$ for all $i \in N$ is roughly 0.5, we set $\mu_i^\rho = 0.4 \times \hat{\mu}_i^\rho$ for all $i \in \{3, 4, 5\}$ and $\mu_i^\rho = 3.45 \times 0.4 \times \hat{\mu}_i^\rho$ for all $i \in \{6, ..., 13\}$ so that the average of μ_i^ρ for all $i \in N$ is also close to 0.5.

B.4 Road Link Capacity

As shown in Section B.2.3, 2,170 tons of supplies from unaffected areas had been sent to Yushu by trucks by 0:00am on April 17, 2010. These supplies were shipped via three road links.[17] Using the unit weight of commodities obtained in Section B.1, we can estimate that 302 units of commodities could be delivered via each road link in 10 days. Therefore, the mean of the road link capacity is set to 300 in Section 4.2.

To estimate the standard deviation, we consider the fact that the roads could be blocked in the earthquake aftermath. It is reported that the roads to Yushu were cleared 6 hours after the earthquake.[18] For the road links within the affected area shown in Figure 2, Table 15 assumes how long deliveries could be interrupted by a shock with a given M_S magnitude. Considering the main shock and the aftershocks occurred within 10 days of the main shock,[19] in the worst case, deliveries

[17] Source: http://news.163.com/10/0415/10/64A8G5L70001124J.html

[18] Source: http://www.sdjt.gov.cn:50080/publish/main/14/2011/20110308212837834253190/20110308212837834253190_.html

[19] Source: http://www.csi.ac.cn/manage/html/4028861611c5c2ba0111c5c558b00001/_content/10_07/27/128019280

could be suspended up to 47 hours, i.e., the delivery capacity would be reduced by 59. Suppose that this worst-case capacity corresponds to the 2.5% percentile of a normally distributed random variable with mean 300. The standard deviation of the road link capacity is 30.

Table 15: Time of delivery interruption caused by shocks

Shock Magnitude (M_S)	≥ 7	$[6, 7)$	$[5, 6)$	< 5
Time of Delivery Interruption (hour)	6	5	4	3

References

[1] Aboolian, R., Cui, T., and Shen, Z.-J.M. (2013). An Efficient Approach for Solving Reliable Facility Location Models. *INFORMS Journal on Computing*, **25(4)**, 720–729.

[2] Altay, N. (2013). Capability-Based Resource Allocation for Effective Disaster Response. *IMA Journal of Management Mathematics*, **24(2)**, 253–266.

[3] Altay, N. and Green, W.G., III. (2006). OR/MS Research in Disaster Operations Management. *European Journal of Operational Research*, **175(1)**, 475–493.

[4] Anaya-Arenas, A.M., Renaud, J., and Ruiz, A. (2014). Relief Distribution Networks: A Systematic Review. *Annals of Operations Research*, **223(1)**, 53–79.

[5] Balcik, B. and Beamon, B.M. (2008). Facility Location in Humanitarian Relief. *International Journal of Logistics: Research and Applications*, **11(2)**, 101–121.

[6] Barbarosoğlu, G. and Arda, Y. (2004). A Two-Stage Stochastic Programming Framework for Transportation Planning in Disaster Response. *Journal of the Operational Research Society*, **55(1)**, 43–53.

[7] Ben-Tal, A., Chung, B.D., Mandala, S.R., and Yao, T. (2011). Robust Optimization for Emergency Logistics Planning: Risk Mitigation in Humanitarian Relief Supply Chains. *Transportation Research Part B: Methodological*, **45(8)**, 1177–1189.

1943.html

[8] Bertsimas, D., and Sim, M. (2004). The Price of Robustness. *Operations Research*, **52(1)**, 35–53.

[9] Bozorgi-Amiri, A., Jabalameli, M.S., and Al-e-Hashem, S.M.J.M. (2013). A Multi-Objective Robust Stochastic Programming Model for Disaster Relief Logistics under Uncertainty. *OR Spectrum*, **35(4)**, 905–933.

[10] Campbell, A.M. and Jones, P.C. (2011). Prepositioning Supplies in Preparation for Disasters. *European Journal of Operational Research*, **209(2)**, 156–165.

[11] Campbell, A.M., Vandenbussche, D., and Hermann, W. (2008). Routing for Relief Efforts. *Transportation Science*, **42(2)**, 127–145.

[12] Dalal, J. and Üster, H. (2017). Combining Worst Case and Average Case Considerations in an Integrated Emergency Response Network Design Problem. *Transportation Science*. Advance online publication. doi:10.1287/trsc.2016.0725.

[13] Davis, L.B., Samanlioglu, F., Qu, X., and Root, S. (2013). Inventory Planning and Coordination in Disaster Relief Efforts. *International Journal of Production Economics*, **141(2)**, 561–573.

[14] Galindo, G. and Batta, R. (2013). Review of Recent Developments in OR/MS Research in Disaster Operations Management. *European Journal of Operational Research*, **230(2)**, 201–211.

[15] Gupta, S., Starr, M.K., Farahani, R.Z., and Matinrad, N. (2016). Disaster Management from a POM Perspective: Mapping a New Domain. *Production and Operations Management*, **25(10)**, 1611–1637.

[16] Haghani, A. and Oh, S.-C. (1996). Formulation and Solution of A Multi-Commodity, Multi-Modal Network Flow Model for Disaster Relief Operations. *Transportation Research Part A: Policy and Practice*, **30(3)**, 231–250.

[17] Holguín-Veras, J., Pérez, N., Jaller, M., Van Wassenhove, L.N., and Aros-Vera, F. (2013). On the Appropriate Objective Function for Post-disaster Humanitarian Logistics Models. *Journal of Operations Management*, **31(5)**, 262–280.

[18] Holguín-Veras, J., Amaya-Leal, J., Cantillo, V., Van Wassenhove, L.N., Aros-Vera, F., and Jaller, M. (2016). Econometric Estimation of Deprivation Cost Functions: A Contingent Valuation Experiment. *Journal of Operations Management*, **45**, 44–56.

[19] Huang, M., Smilowitz, K.R., and Balcik, B. (2013). A Continuous Approximation Approach for Assessment Routing in Disaster Relief. *Transportation Research Part B: Methodological*, **50**, 20–41.

[20] Jia, H., Ordóñez, F., and Dessouky, M. (2007). A Modeling Framework for Facility Location of Medical Services for Large-Scale Emergencies. *IIE Transactions*, **39(1)**, 41–55.

[21] Lee, E.K., Chen, C.-H., Pietz, F., and Benecke, B. (2009). Modeling and Optimizing the Public-Health Infrastructure for Emergency Response. *Interfaces*, **39(5)**, 476–490.

[22] Liu, B., Lee, S.-J., Jiao, Z., and Wang, L. (2011). *Contemporary Logistics in China: An Introduction*. World Scientific.

[23] Mete, H.O. and Zabinsky, Z.B. (2010). Stochastic Optimization of Medical Supply Location and Distribution in Disaster Management. *International Journal of Production Economics*, **126(1)**, 76–84.

[24] Najafi, M., Eshghi, K., and Dullaert, W. (2013). A Multi-Objective Robust Optimization Model for Logistics Planning in the Earthquake Response Phase. *Transportation Research Part E: Logistics and Transportation Review*, **49(1)**, 217–249.

[25] Özdamar, L., Ekinci, E., and Küçükyazici, B. (2004). Emergency Logistics Planning in Natural Disasters. *Annals of Operations Research*, **129(1)**, 217–245.

[26] Qi, L., Shen, Z.-J.M., and Snyder, L.V. (2010). The Effect of Supply Disruptions on Supply Chain Design Decisions. *Transportation Science*, **44(2)**, 274–289.

[27] Rawls, C.G. and Turnquist, M.A. (2010). Pre-Positioning of Emergency Supplies for Disaster Response. *Transportation Research Part B: Methodological*, **44(4)**, 521–534.

[28] Rawls, C.G. and Turnquist, M.A. (2011). Pre-Positioning Planning for Emergency Response with Service Quality Constraints. *OR Spectrum*, **33(3)**, 481–498.

[29] Salmerón, J. and Apte, A. (2010). Stochastic Optimization for Natural Disaster Asset Prepositioning. *Production and Operations Management*, **19(5)**, 561–574.

[30] Shen, Z.-J.M., Zhan, R.L., and Zhang, J. (2011). The Reliable Facility Location Problem: Formulations, Heuristics, and Approximation Algorithms. *INFORMS Journal on Computing*, **23(3)**, 470–482.

[31] Sheu, J.-B. (2007). An Emergency Logistics Distribution Approach for Quick Response to Urgent Relief Demand in Disasters. *Transportation Research Part E: Logistics and Transportation Review*, **43(6)**, 687–709.

[32] Sheu, J.-B. (2010). Dynamic Relief-Demand Management for Emergency Logistics Operations under Large-Scale Disasters. *Transportation Research Part E: Logistics and Transportation Review*, **46(1)**, 1–17.

[33] Shu, J. (2010). An Efficient Greedy Heuristic for Warehouse-Retailer Network Design Optimization. *Transportation Science*, **44(2)**, 183–192.

[34] Simpson, N.C. and Hancock, P.G. (2009). Fifty Years of Operational Research and Emergency Response. *Journal of the Operational Research Society*, **60(S1)**, S126–S139.

[35] Soyster, A.L. (1973). Convex Programming with Set-Inclusive Constraints and Applications to Inexact Linear Programming. *Operations Research*, **21(5)**, 1154–1157.

[36] Toregas, C., Swain, R., ReVelle, C., and Bergman, L. (1971). The Location of Emergency Service Facilities. *Operations Research*, **19(6)**, 1363–1373.

[37] Tufekci, S. and Wallace, W.A. (1998). The Emerging Area of Emergency Management and Engineering. *IEEE Transactions on Engineering Management*, **45(2)**, 103–105.

[38] Tzeng, G.-H., Cheng, H.-J., and Huang, T.D. (2007). Multi-Objective Optimal Planning for Designing Relief Delivery Systems. *Transportation Research Part E: Logistics and Transportation Review*, **43(6)**, 673–686.

[39] Wang, Y. (2010). Study on Cost Estimation Method of Post-Earthquake Rehabilitation. Ph.D. Thesis, Institute of Engineering Mechanics, China Earthquake Administration, Harbin, China.

[40] Xu, G., Yuan, Y., Fang, W., and Shi, P. (2011). Fast Loss Assessment of M7.1 Yushu Earthquake. *Journal of Earthquake Engineering and Engineering Vibration*, **31(1)**, 114–123.

[41] Yushimito, W.F., Jaller, M., and Ukkusuri, S. (2012). A Voronoi-Based Heuristic Algorithm for Locating Distribution Centers in Disasters. *Networks and Spatial Economics*, **12(1)**, 21–39.